

Structure–Activity Relationships of Monomeric C2-Aryl Pyrrolo[2,1-*c*][1,4]benzodiazepine (PBD) Antitumor Agents

Dyeison Antonow,^{†,‡} Maciej Kaliszczak,[§] Gyoung-Dong Kang,[‡] Marissa Coffils,[‡] Arnaud C. Tiberghien,[‡] Nectaroula Cooper,[†] Teresa Barata,[†] Sibylle Heidelberger,[†] Colin H. James,[†] Mire Zloh,[†] Terence C. Jenkins,^{||} Anthony P. Reszka,[⊥] Stephen Neidle,[⊥] Sylvie M. Guichard,[§] Duncan I. Jodrell,^{§,∇} John A. Hartley,[#] Philip W. Howard,^{*,†,‡} and David E. Thurston^{*,†,‡}

[†]Cancer Research UK Gene Targeted Drug Design Research Group, The School of Pharmacy, University of London, 29/39 Brunswick Square, London WC1N 1AX, U.K., [‡]Spirogen Ltd, 29/39 Brunswick Square, London WC1N 1AX, U.K., [§]Cancer Research UK Pharmacology and Drug Development Group, University of Edinburgh Cancer Research Centre, Crewe Road, Edinburgh EH4 2XR, U.K., ^{||}Morvus Technology Limited, Tŷ Myddfai, Llanarthne, Carmarthen SA32 8HZ, U.K., [⊥]Cancer Research UK Biomolecular Structure Research Group, The School of Pharmacy, University of London, 29/39 Brunswick Square, London WC1N 1AX, U.K., and [#]Cancer Research UK Drug–DNA Interactions Research Group, UCL Cancer Institute, 72 Huntley Street, London WC1E 6BT, U.K. [∇]Current address: Cancer Research UK Cambridge Research Institute, University of Cambridge.

Received November 21, 2009

A comprehensive SAR investigation of the C2-position of pyrrolo[2,1-*c*][1,4]benzodiazepine (PBD) monomer antitumor agents is reported, establishing the molecular requirements for optimal in vitro cytotoxicity and DNA-binding affinity. Both carbocyclic and heterocyclic C2-aryl substituents have been studied ranging from single aryl rings to fused ring systems, and also styryl substituents, establishing across a library of 80 analogues that C2-aryl and styryl substituents significantly enhance both DNA-binding affinity and in vitro cytotoxicity, with a correlation between the two. The optimal C2-grouping for both DNA-binding affinity and cytotoxicity was found to be the C2-quinolinyl moiety which, according to molecular modeling, is due to the overall fit of the molecule in the DNA minor groove, and potential specific contacts with functional groups in the floor and walls of the groove. This analogue (**14i**) was shown to delay tumor growth in a HCT-116 (bowel) human tumor xenograft model.

Introduction

Naturally occurring pyrrolo[2,1-*c*][1,4]benzodiazepine (PBD)^a compounds are isolated from the fermentation broth of *Streptomyces* species and are known for their antibiotic and antitumor properties.^{1,2} They can exist as N10–C11 carbinoamine methyl ethers (e.g., anthramycin, **1**), carbinolamines (e.g., sibiromycin, **2**), or imines (e.g., the synthetic C2-aryl PBD-imines, **3**, **4**, and **5**), although these different forms can interconvert at the N10–C11 position depending on solvent and isolation conditions (Figure 1). However, in all cases, the C11-position is electrophilic and enables the molecules to alkylate the NH₂ group of a guanine in the minor groove of DNA.¹ This reaction is sequence-selective and preferentially targets 5'-Pu-G-Pu sequences. The PBDs have a right-handed twist due to the “S”-configuration at their C11a-position, which allows them to fit perfectly within the DNA minor groove. These properties differentiate PBDs from other families of DNA-

alkylating agents, and both the chemical and biological aspects of these compounds have been explored by several research groups since the discovery of anthramycin in the 1960s.^{3–20}

Structure–activity relationship (SAR) information for the PBDs was initially established based on biological data obtained from natural compounds.^{21–23} The development of an understanding of their mode of action prompted the rational design of synthetic analogues which provided additional chemical and biological information.^{1,2} The recent growth of interest in PBDs is partly due to the progress of SJG-136, which is the first synthetic PBD-based compound to enter phase II clinical trials with success.^{24–27} Joining two PBD monomeric units together to make PBD dimers such as SJG-136 results in greater in vitro cytotoxicity and in vivo antitumor efficacy due to the ability of these molecules to cross-link DNA.^{25,28} However, PBD dimer syntheses are generally lengthier than those for PBD monomers, and this has limited the scope for structural diversification. Since the success of SJG-136, there has been interest in progressing a PBD monomer to clinical trials due to the potential advantages including lower molecular weight, ease of synthesis, and greater potential for structural diversification. In addition, compared to PBD dimers, the monomers are poor substrates for ABC transporters²⁹ which can lead to multidrug resistance in a clinical setting. For example, SJG-136 is a substrate for the ABC transporter P-glycoprotein (ABCBI/P-gp).^{30,31} Also, other preclinical data³² indicate that, as a class, C2-modified PBD monomers have in vivo antitumor activity in

*To whom correspondence should be addressed. Phone: +44 (0) 207 753 5932. Fax: +44 (0) 207 753 5965. E-mail: philip.howard@spirogen.com (P.W.H.); david.thurston@pharmacy.ac.uk (D.E.T.).

^aAbbreviations: BAIB, [bis(acetoxy)iodo]benzene; CT-DNA, calf thymus DNA; ΔT_m , enhancement in thermal denaturation temperature of calf-thymus DNA; EDCI, 1-ethyl-3-(3-dimethylaminopropyl) carbodiimide hydrochloride salt; HCT-116, human colorectal tumor cell line; NaHMDS, sodium bis(trimethylsilyl)amide; 2D NOESY two-dimensional nuclear Overhauser enhancement spectroscopy; PBD, pyrrolo[2,1-*c*][1,4]benzodiazepine; Pu, purine nucleotides; SAR, structure–activity relationship; TEMPO, 2,2,6,6-tetramethylpiperidine-1-oxyl; TLC, thin layer chromatography.

mouse models, thus providing the basis for translational studies toward a phase I clinical trial.

In a previous study of synthetic PBD monomers, we found that introduction of an aryl group at the 2-position significantly enhanced in vitro cytotoxicity.³³ The role played by the additional aryl fragment was not fully understood at the time and prompted the detailed study reported here. In related work, we established³⁴ that a series of C2-aryl PBD dilactams devoid of A-ring substituents and lacking a DNA-alkylating N10–C11 imine moiety had enhanced DNA-binding affinity compared to the parent non-C2-substituted PBD dilactam, elevating the melting temperature of double-stranded calf thymus DNA by up to 2.3 °C after 18 h incubation and thus confirming the importance of the C2-substituent in stabilizing DNA interaction. In a follow-up study we reported the synthesis of a novel C2-aryl PBD-imine library in which a parallel approach was employed to obtain 66 structurally unique C2-aryl-substituted PBDs containing A-ring electron-donating substituents and N10–C11 imine functionalities.³⁵ We also reported a synthetic

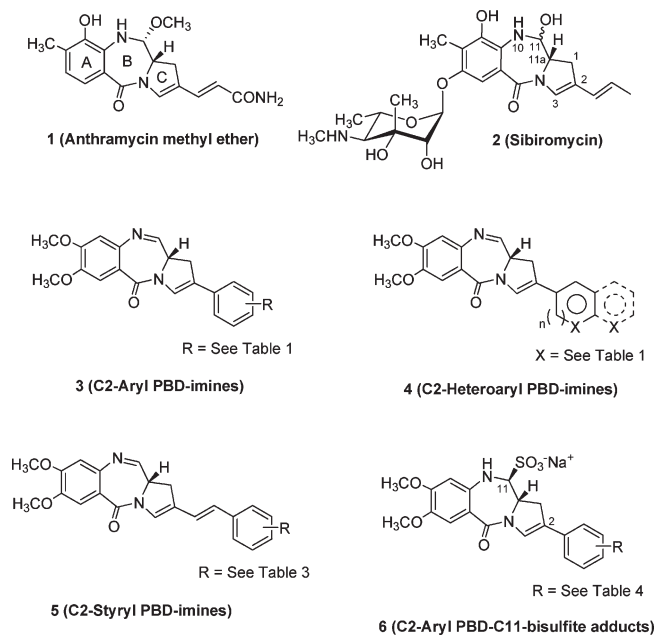


Figure 1. Structures of the naturally occurring PBD monomers anthramycin (**1**), sibiromycin (**2**), and the novel synthetic C2-substituted PBD analogues (**4–6**).

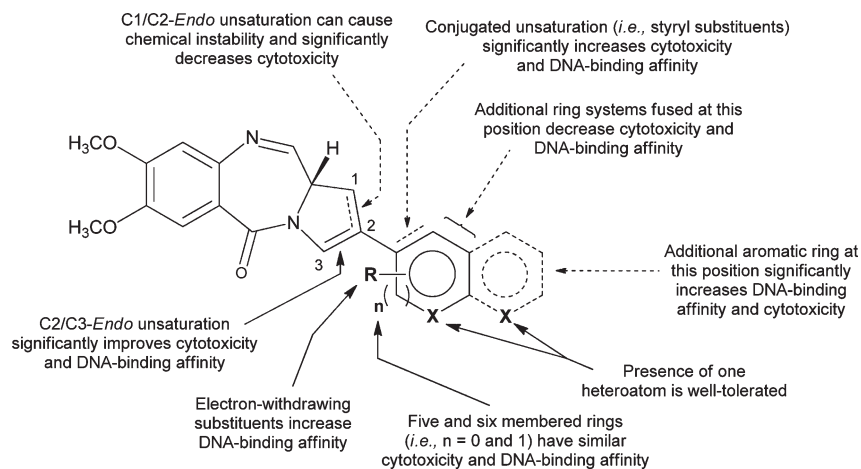


Figure 2. Summary of SARs for the C2-aryl functionalization of PBD monomers based on in vitro cytotoxicity, DNA thermal denaturation, and NMR data.

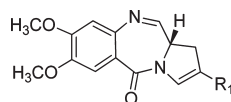
procedure to obtain C1/C2-endo-unsaturated C2-aryl PBD imines.³⁶

We now report biological (in vitro cytotoxicity and xenograft) and biophysical (DNA thermal denaturation) data for a library of 80 C2-aryl-substituted PBD-imine compounds synthesized via three different routes. The library includes a number of novel C2-heteroaryl and C2-styryl analogues, and some C1/C2-endo-unsaturated C2-aryl PBD analogues (Tables 1 and 3). A synthetic route to a novel C-ring saturated C2-aryl PBD (i.e., **27**, Scheme 2) is also described, thus providing an important “control” molecule along with further insights into the SAR of PBD monomers (Figure 2). Molecular modeling studies have been used to examine the DNA-binding of key members of the series. Furthermore, the water solubility of some analogues has been dramatically improved by converting to C11-(sodium bisulfite) adducts (i.e., **6**, Figure 1). Finally, one library member (**14i**) has been evaluated in a HCT-116 human tumor xenograft model and shown to have in vivo antitumor activity.

Results and Discussion

Chemistry. Synthesis of C2/C3-endo-Unsaturated C2-Aryl and C2-Styryl PBD Imines (Scheme 1, and Tables 1 and 3). The C2-aryl PBDs were originally synthesized according to the reductive cyclization approach developed by Leimgruber and co-workers.³⁷ We initially reported³³ application of the Suzuki reaction to introduce aryl substituents at the same position employing aryl boronic acids and C2-enol triflate PBDs. Subsequently, we reported the use of Stille coupling to install vinyl and heteroaryl substituents at the C2-position of PBDs³⁸ [The Supporting Information document contains full synthetic methodologies and characterization data for the Stille and Suzuki coupling products previously reported only in communications]. More recently, we reported the parallel synthesis of 66 C2-aryl-modified PBDs via palladium catalyzed cross-coupling.³⁵ This parallel approach allowed the rapid synthesis of a set of N10–C11 imine-containing C2-substituted PBDs with stereochemical integrity at their C11a-position. The same methodology was used in this study (Scheme 1) for the synthesis of the novel PBDs included in the sublibraries contained in **8–15** (Table 1)³⁵ and the C2-styryl sublibrary **16a–e** (Table 3).

Synthesis of C1/C2-endo-Unsaturated and Fully-Saturated C-Ring C2-Substituted PBD Imines (Scheme 2, Table 1). The effect of the location of unsaturation (i.e., C1–C2 or

Table 1. Cytotoxicity Data for the C2-Aryl PBD Library^a

Compound Number	R ₁	NCI Screen (μM) ^d			K562 (μM) ^b IC ₅₀	Compound Number	R ₁	NCI Screen (μM) ^d			K562 (μM) ^b IC ₅₀
		GI ₅₀	TGI	LC ₅₀				GI ₅₀	TGI	LC ₅₀	
C2-phenyl											
(8)		0.002	0.04	5.13	0.0025						
Para-substituted C2-phenyl											
(9a)		0.003	0.04	3.23	0.0321	(9o)		0.002	0.07	4.47	0.0313
(9b)		0.002	0.03	4.79	0.0140	(9p)		---	---	---	0.2366
(9c)		0.006	0.20	11.5	0.0297	(9q)		0.009	0.16	15.1	0.0263
(9d)		0.002	0.08	3.39	0.0103	(9r)		0.004	0.03	1.66	0.0243
(9e)		0.001	0.15	19.0	0.0049	(9s)		0.003	0.15	7.41	0.0198
(9f)		0.003	0.03	1.26	0.0511	(9t)		13.2	23.4	25.1	>1.0
(9g)		0.002	0.05	1.94	0.0478	(9u)		0.004	0.07	6.92	0.0131
(9h)		0.002	0.18	8.90	0.00028	(9v)		0.009	0.46	13.8	0.0156
(9i)		0.001	0.07	4.17	0.0795	(9w)		0.015	0.71	13.8	0.0595
(9j)		0.004	0.06	4.46	0.1151	(9x)		0.158	1.86	12.6	0.1607
(9k)		0.005	0.01	0.62	0.0690	(9y)		0.019	0.09	3.89	0.1140
(9l)		0.008	0.09	3.63	0.0196	(9z)		0.058	0.83	35.5	0.1650
(9m)		0.005	0.02	1.44	0.0190	(9a')		0.005	0.08	8.32	0.00063
(9n)		0.002	0.12	11.2	0.0016	(9b')		0.005	0.16	13.2	0.0088
Meta-substituted C2-phenyl											
(10a)		0.004	0.05	5.89	0.0595	(10h)		0.004	0.56	16.2	0.0151
(10b)		0.011	0.06	4.07	0.00045	(10i)		---	---	---	>1.0
(10c)		0.005	0.07	7.58	0.0095	(10j)		0.005	0.04	7.58	0.0124
(10d)		0.003	0.05	16.6	0.0064	(10k)		0.005	0.05	5.62	0.0581
(10e)		0.017	0.10	0.54	0.0194	(10l)		0.027	1.86	10.5	0.1190
(10f)		0.006	0.03	1.35	0.0468	(10m)		0.102	0.85	14.1	0.2730
(10g)		0.006	0.18	7.24	0.0765						

Table 1. Continued

Compound Number	R ₁	NCI Screen (μM) ^a			K562 (μM) ^b IC ₅₀	Compound Number	R ₁	NCI Screen (μM) ^a			K562 (μM) ^b IC ₅₀
		GI ₅₀	TGI	LC ₅₀				GI ₅₀	TGI	LC ₅₀	
Ortho-substituted C2-phenyl											
(11a)		0.012	0.25	10.7	0.0093	(11b)		0.016	0.16	4.36	0.2580
Di-substituted C2-phenyl											
(12a)		0.110	1.10	11.7	0.0610	(12c)		0.025	0.33	4.36	0.0071
(12b)		0.851	3.46	20.9	>1.0	(12d)		0.003	0.05	3.02	0.1060
C2-Naphthyl											
(13a)		0.0006	0.015	0.40	0.0454	(13c)		0.002	0.02	1.95	0.0126
(13b)		0.0009	0.007	0.27	0.0023	(13d)		0.138	0.95	13.9	0.5724
C2-Heteroaryl											
(14a)		0.010	0.15	0.74	0.0011	(14g)		0.006	0.05	0.44	0.0108
(14b)		0.012	0.27	6.46	0.0201	(14h)		0.005	0.09	0.54	0.0267
(14c)		0.003	0.05	5.37	0.0122	(14i)		0.002	0.03	3.63	0.00047
(14d)		0.005	0.07	17.0	0.0182	(14j)		0.005	0.04	7.08	0.0126
(14e)		0.018	0.60	26.9	0.0287	(14k)		0.0001	0.001	0.18	0.0089
(14f)		0.004	0.06	4.07	0.0094	(14l)		0.0004	0.004	0.19	0.0014
C2-(Tricyclic) heteroaryl and C2-pyrenyl analogues											
(15a)		0.025	0.22	5.37	0.1633	(15c)		0.501	1.74	8.91	>1.0
(15b)		0.049	0.21	2.82	0.1616	(15d)		0.398	1.44	10.7	0.0862
C1/C2-Endo-unsaturated and fully saturated C-ring C2-aryl PBDs											
29 ³⁶		0.102	0.45	0.91	0.9400	27		9.77	43.65	91.20	>1.0
Comparative Data											
30 ³⁹		2.138	19.0	57.5	0.4880	31 ³⁸		1.35	8.13	60.2	0.0144
Anthramycin methyl ether (1)		0.013	1.58	24.5	0.0080	Sibiromycin (2)		0.033	0.85	16.7	0.0014

^a NCI 60 cell-line panel. Figures correspond to the mean values (MG-MID) calculated from the 60 individual cell lines (see Supporting Information).

^b K562 human chronic myeloid leukemia cell line (96 h incubation, see Experimental Section).

C2–C3) in the PBD C-ring on biological potency has been unclear to date. Therefore, we prepared examples of both for evaluation. We found that a C1/C2-enol-triflate analogue of

7 could be obtained under kinetic conditions which allowed further elaboration to C2-aryl PBDs (e.g., 29, Table 1) via Suzuki coupling.³⁶ To fully understand the impact of

Table 2. Selected Thermal Denaturation (ΔT_m) Values for Representative PBD Imine Library Members

Compd		Induced ΔT_m ($^{\circ}\text{C}$) ^a		
no.	C2-substituent	0 h	4 h	18 h
12b ^b	(phenyl) 2,6-CH ₃	0.5 ^c	0.5 ^c	0.5 ^c
9b	(phenyl) 4-NH ₂	5.8	6.2	6.5
11a	(phenyl) 2-CH ₃	6.2	6.8	6.9
9j	(phenyl) 4-CH(CH ₃) ₂	6.5	6.7	6.9
9a	(phenyl) 4-N(CH ₃) ₂	6.9	7.6	8.0
9l	(phenyl) 4-Ph	8.0	8.1	8.4
9g	(phenyl) 4-C(CH ₃) ₃	8.7	9.0	9.2
9k	(phenyl) 4-CHCH ₂	8.5	9.0	9.2
9i	(phenyl) 4-CH ₂ CH ₃	9.0	9.4	9.7
10b	(phenyl) 3-OCH ₃	9.8	10.1	10.2
9o	(phenyl) 4-Cl	9.6	9.9	10.2
14i	(phenyl) 3,4-OCH ₂ O	9.9	10.3	10.3
9h	(phenyl) 4-CH ₃	9.4	9.7	10.1
9e	(phenyl) 4-OCH ₃	10.2	10.5	10.6
9n	(phenyl) 4-F	10.1	10.4	10.6
9m	(phenyl) 4-SCH ₃	10.4	10.5	10.7
9q	(phenyl) 4-CHO	10.4	10.6	10.8
8	(phenyl) 4-H	10.5	10.6	10.8
9s	(phenyl) 4-CN	10.7	10.9	11.0
9r	(phenyl) 4-CF ₃	11.4	11.7	11.9
9f	(phenyl) 4-OPh	11.5	11.9	12.1
14a	2-thiophenyl	12.0	12.7	13.0
13a	2-naphthyl	14.8	15.4	15.7
14k	3-quinoliny	17.7	18.1	18.2
14l	6-quinoliny	19.1	19.9	20.5
anthramycin methyl ether (1) ⁴⁷		9.4	11.2	13.0
sibiromycin (2) ⁴⁷		15.7	16.0	16.3

^a See Experimental Section for details. ^b This compound was synthesized according to ref 33. ^c Values for this compound were measured in a different laboratory using 10 mM NaH₂PO₄/Na₂HPO₄ and 1 mM Na₄EDTA as buffer, rather than the 10 mM NaH₂PO₄/Na₂HPO₄ and 1 mM Na₂EDTA used for studies with all other compounds. The higher [Na⁺] and increased ionic strength for this buffer is reflected in a higher T_m value for the native CT-DNA (i.e., T_m (DNA) = 70.63 $^{\circ}\text{C}$ rather than 67.82 $^{\circ}\text{C}$). Further, 20 μM **12b** and higher 200 μM DNA (in DNAP, equivalent to 100 μM in base pairs [bp]) was used. This 1:10 [ligand]/[DNAP] molar ratio compares with the 1:5 ratio used for all other compounds. Using this high-[Na⁺] buffer and a 1:10 molar ratio, anthramycin methyl ether (**1**) gave corresponding ΔT_m shifts of 13.70, 14.17 and 14.08 $^{\circ}\text{C}$, at 0, 4 and 18 h, respectively.

unsaturation in the C-ring, we also synthesized the novel fully saturated C2-aryl PBD-imine **27** (Scheme 2). The synthesis started from the C-ring building block **17**,³⁹ which was oxidized to the C2-ketone (**18**) using TEMPO and BAIB. The enol-triflate **19** was obtained in excellent yield (91%) via kinetic enolisation of **18** using NaHMDS. Suzuki coupling was performed next on the C-ring building block before attachment to the nitrobenzoyl fragment (A-ring precursor). This strategy allowed the use of hydrogenation for selective reduction of the *endo*-unsaturation in the pyrrolidine ring. The cross-coupled product **20** was exposed to H₂ in the presence of catalytic amounts of palladium on charcoal to simultaneously deprotect the cyclic amine and reduce the *endo*-unsaturation in stereospecific fashion. Next, the C-ring building block **21** was coupled to 2-nitroveratric acid, and the product further elaborated to the N10-Alloc-protected PBD **26** using standard synthetic methods. Final deprotection with Pd(PPh₃)₄ afforded the novel C2-substituted C-ring saturated PBD-imine **27** which was characterized by 2D-NOESY NMR (see Supporting Information).

Synthesis and C11-Stereochemistry of C2-Aryl PBD C11-(Sodium Bisulfite) Adducts (Scheme 3, Table 4). C11-(Sodium

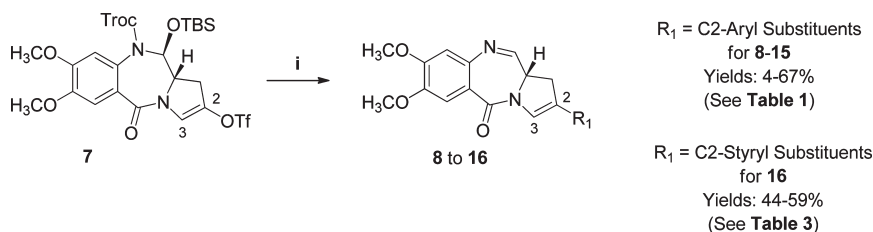
Table 3. Cytotoxicity Data for the C2-Styryl Analogues

Number	Compound R ₁	NCI Screen (μM) ^a			K562 IC ₅₀ ^b (μM)
		GI ₅₀	TGI	LC ₅₀	
16a		0.004	0.02	1.58	<0.0001
16b		0.002	0.05	0.44	0.0411
16c		0.005	0.01	1.10	0.00013
16d		0.005	0.02	1.00	0.0154
16e		0.003	0.02	1.10	0.0312
Comparative Data					
32 ³⁸		0.078	1.23	30.2	0.0027

^a NCI 60 cell-line panel. Figures correspond to the mean values (MG-MID) calculated from the 60 individual cell lines (see Supporting Information). ^b K562 human chronic myeloid leukemia cell line (96 h incubation, see Experimental Section).

bisulfite) adducts (**28a–f**, Scheme 3) were prepared to improve the water solubility of the C2-aryl PBDs. PBD-bisulfite adducts were originally reported by Kaneko and co-workers⁴⁰ and were shown to have greater chemical stability than their parent N10–C11 imines. Later, Langlois and co-workers reported the synthesis of an anthramycin-related analogue containing a C11-bisulfite moiety.⁴¹ However, in neither case was the stereochemistry of the C11–SO₃[−]Na⁺ linkage assigned.

We initially utilized Langlois' method but with modified reaction conditions in terms of time and solvent composition, which proved to be efficient for the synthesis of C2-aryl PBD C11-sodium bisulfite adducts. The straightforward workup, involving simple extraction into deionized water, gave the adducts as solids following lyophilization. Because the stereochemistry of C11-bisulfite adducts had not been studied by either Kaneko or Langlois, we carried out a comprehensive NMR investigation in both DMSO-*d*₆ and D₂O solutions. Using compound **28d** as an example, we found that the C11*S*-(sodium bisulfite) adduct is the major species and that its formation is affected by solvent composition and reaction time [NOTE: The ¹H NMR in DMSO-*d*₆ showed a doublet ($J = 10.4$ Hz) at 3.96 ppm corresponding to the H11-proton, the strong coupling indicating that this proton was positioned in an "anti" orientation relative to H11a.¹ The C11*R*-(sodium bisulfite) addition product was not observed by NMR under these conditions (see Supporting Information for ¹H- and 2D-NMR spectra)]. Further NMR analysis including COSY and NOESY experiments indicated the presence of the N10–C11 hydrolysis product (i.e., B-ring opened aldehyde) (Figure 3) [NOTE: There is a significant change in the chemical environment of the H1 protons upon B-ring closure. As a consequence, H1 α and H1 β become less shielded in the PBD ring system]. Interestingly, the ratio of products changed when a mixture of 2-propanol-*d*₈/D₂O (2:1 v/v) was used as solvent.⁸ In this

Scheme 1. C2/C3-*Endo*-Unsaturated C2-Aryl PBDs Obtained via the Parallel Approach.^a

^a Reagents and conditions: (i) PS-PPh₃Pd (0.01 equiv), boronic acid 1.1 equiv, TEA (6.0 equiv), 100 °C (microwave radiation), 10 min; then 10% Cd/Pb (8.0 equiv), 1 M NH₄OAc/THF (2:3), rt, 0.5 to 2.5 h, 4 to 67%. See Ref 35 for full analytical data and experimental details for **8–15**. Analytical data for novel compounds **14k**, **14l**, and **16** are provided in Supporting Information.

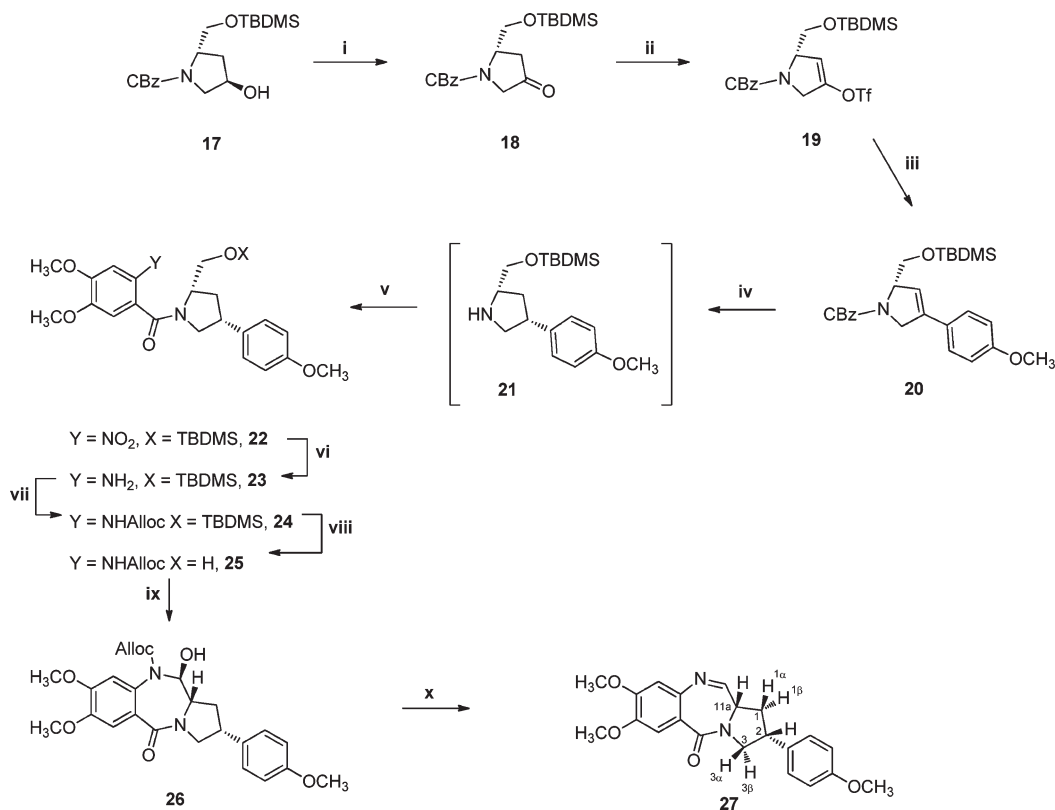
case, formation of the C11S-bisulfite was maximized, and only a negligible amount of B-ring-opened product was observed. ¹H NMR time-course experiments were also carried out using the biphasic system D₂O/CD₂Cl₂ (1:1 v/v) as solvent (see Supporting Information). The results suggested that, under the acidic conditions (pH 5) of the aqueous sodium bisulfite layer, the PBD-imine initially dissolved in the organic phase and then became protonated to form an iminium species which reacted with excess water to give the N10–C11 carbinolamine as the predominant species. Carbinolamines of this type have been reported to exist in equilibrium with their equivalent ring-opened amino-aldehyde forms.⁴² This aldehyde species can in turn react with bisulfite anion to give the B-ring-opened bisulfite adduct, although this product was only observed at early reaction times (i.e., 1–5 min, see Supporting Information) and presumably rapidly interconverts back to the cyclized C11S-bisulfite product according to the equilibrium shown in Figure 3. The presence of these interconverting forms was further supported by “trapping” the PBD-imine form in the organic layer. This was carried out by shaking a D₂O solution of an imine-free lyophilized sample of the isolated PBD-bisulfite adduct **28d** with CD₂Cl₂, followed by phase separation and ¹H NMR analysis, which clearly showed the presence of the PBD-imine species (i.e., ¹H NMR spectrum identical to **10b**).

Biological and Biophysical Data. In Vitro Cytotoxicity. All library members were evaluated for cytotoxicity across the NCI 60 cell-line panel (see Supporting Information) and the K562 leukemia cell line. The NCI screen was repeated after a period of 2–3 months with the majority of compounds retaining their cytotoxicity properties, thus providing an indication of their chemical stability. The most noticeable observation from the NCI data was the selective cytotoxicity of the C2-aryl PBD imines towards melanoma cell lines. Compounds with C1/C2-*endo* unsaturation (e.g., **29**) and/or a fully saturated C-ring (i.e., **27**) were either significantly less cytotoxic than the equivalent C2/C3-*endo*-unsaturated molecules or completely inactive (Table 1). Molecular modeling analysis involving a conformational search (MacroModel, version 9.6) indicated that **27** and **29** are unlikely to bind effectively to double-stranded DNA (a model 14-mer DNA duplex⁴³ was studied; data not shown) due to their overall shape and lack of isohelicity with the DNA minor groove. In addition, it was observed that **29** is prone to undergo C-ring aromatization³⁶ which may also reduce its overall cytotoxicity. In vitro data generated for the parallel-synthesized C2/C3-*endo*-unsaturated C2-aryl and C2-styryl PBD imines, and the PBD C11-(sodium bisulfite) adducts are collected in Tables 1, 3, and 4).

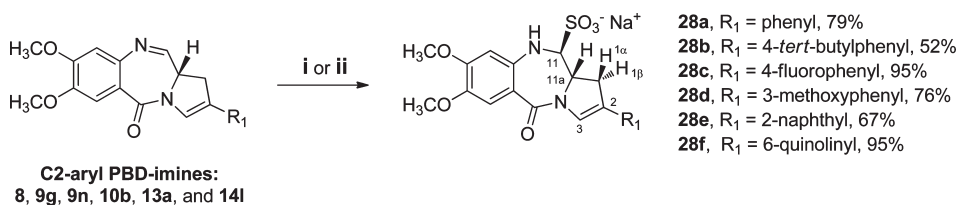
DNA Thermal Denaturation Studies. Reactivity of the C2-aryl PBD monomers toward double-stranded DNA was assessed by measuring their induced effects on the melting behavior (T_m) of duplex-form calf thymus DNA.^{44,45} Thermal denaturation data for selected members of the PBD imine library are shown in Table 2. C2-Substituted PBD imines were found to shift the DNA melting curve significantly (stabilization) compared to PBD dilactams,^{34,44} highlighting the importance of the N10–C11 imine functionality, the 7- and 8-OCH₃ A-ring substituents, and the C2-aryl functionalities on DNA-binding affinity. A number of trends are apparent from Table 2 for simple C2-phenyl substituted compounds. First, the addition of two *ortho*-methyl substituents to the simple C2-phenyl group (**12b**) reduces DNA stabilization significantly ($\Delta T_m = 0.5$ °C). On the other hand, electron-withdrawing groups appear to be more favorable than electron-donators in enhancing binding affinity in the *para*-substituted analogues (See Table S1, Supporting Information). For example, **9r** (4-CF₃, $\Delta T_m = 11.9$ °C) and **9s** (4-CN, $\Delta T_m = 11.0$ °C) provide greater DNA stabilization than **9h** (4-CH₃, $\Delta T_m = 10.1$ °C) or **9e** (4-OCH₃, $\Delta T_m = 10.6$ °C). However, fused carbocyclic and heterocyclic six-membered ring systems provide the greatest degree of stabilization, with **13a** (2-naphthyl), **14k** (3-quinoliny), and **14l** (6-quinoliny), stabilizing the double helix by 15.7, 18.2, and 20.5 °C, respectively. These high values are remarkable in that they are in the range of ΔT_m values associated with PBD dimer molecules such as DSB-120 ($\Delta T_m = 15.1$ °C, under identical conditions),⁴⁶ which covalently cross-link the two DNA strands in an interstrand manner.

Structure–Activity Relationships (SARs). The importance of C2-aryl-substituents and a sp² carbon at the C2-position can be seen in naturally occurring PBDs with the C2-functionalizations of anthramycin (**1**) and sibiromycin (**2**), two of the most potent PBD natural products known. It is also evident from the range of known natural products that these changes to the C-ring can lead to greater cytotoxicity enhancement than A-ring modifications.⁴⁷ With C2-sp² compared to C2-sp³ functionalization, the molecules adopt a flatter overall structure and a conformation more favorable for interacting in the DNA minor groove through maximal intermolecular hydrogen bonding, electrostatic, and van der Waals interactions. We have previously synthesized^{38,48,49} C2/C3-*endo*-unsaturated PBD-imines with average in vitro potencies higher than anthramycin.

The high potency associated with many of the compounds in this study was “off scale” in the NCI’s high-throughput cytotoxicity assay. Hence, we focused our SAR analysis mainly on the IC₅₀ values obtained from the K562 cell line. Cytotoxicity

Scheme 2. Fully Saturated C2-Aryl PBD (**27**) Obtained via Suzuki Coupling between the Pyrrolidinic Enol-triflate **19** and 4-Methoxyphenylboronic Acid^a

^a Reagents and conditions: (i) TEMPO (0.1 equiv), BAIB (1.1 equiv), CH₂Cl₂, rt, 2 h, 48%; (ii) NaHMDS (1.1 equiv), THF, -78 °C, 1.5 h, then *N,N*-bis(trifluoromethanesulfonyl)anilide (1.1 equiv), 91%; (iii) 4-methoxyphenyl boronic acid (1.0 equiv), Pd(PPh₃)₄ (0.01 equiv), aq Na₂CO₃, toluene, rt, 36 h, 45%; (iv) 10% Pd/C, EtOH, H₂, rt 12 h, 99%; (v) 4,5-dimethoxy-2-nitrobenzoic acid, EDCI, 1.2 equiv, HOBT (1.2 equiv), CH₂Cl₂, 0 °C, 2 h, 74%; (vi) 10% Pd/C, EtOH, H₂, rt 12 h, 72%; (vii) Alloc-Cl (1.5 equiv), pyridine (2.2 equiv), CH₂Cl₂, rt, 6 h, 82%; (viii) TBAF (1.2 equiv), THF, rt 3 h, 96%; (ix) TEMPO (0.1 equiv), BAIB (1.1 equiv), CH₂Cl₂, rt, 5 h, 65%; (x) Pd(PPh₃)₄ (0.01 equiv), pyrrolidine (1.1 equiv), CH₂Cl₂, rt, 30 min, 58%.

Scheme 3. Synthesis of C2-Aryl PBD C11-(Sodium Bisulfite) Adducts^a

^a Reagents and conditions: (i) CH₂Cl₂/water (1:1 v/v), aq NaHSO₃ (1.1 equiv), rt, 5 to 80 min; (ii) 2-propanol/water (2:1 v/v), aq NaHSO₃ (1.1 equiv), rt, 5 min (See Supporting Information). ^b Yields refer to reaction conditions (i).

values for the C2-aryl and styryl PBDs (Tables 1 and 3) exhibited a wide range from <0.1 to 920 nM. In general, compounds with the highest ΔT_m values had the lowest IC₅₀ values, however this correlation was not perfect due to the wide structural diversity of the compounds ($r^2=0.33$, $P_{\text{value}}=0.0014$). Several physicochemical properties were investigated using Chem3D 11.0 (CambridgeSoft) in an attempt to identify parameters that might better correlate with cytotoxicity. Interestingly, we found a statistically significant correlation between solvent accessible surface area (SASA) and cytotoxicity ($r^2=0.81$, $P_{\text{value}}<0.0001$).

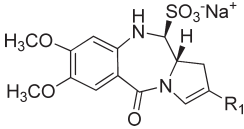
C2-Aryl PBD Imines. There is no significant difference between the IC₅₀ values of compounds in the C2-phenyl series (Table 1) for different substituents in the ortho, meta, and para positions, although a clear trend is noticeable within the *para*- and *meta*-halogenated series (i.e., **9n–o**

and **10d–e**) which may reflect the electronegativity or bulkiness of the substituents. However, introduction of long aliphatic moieties protruding from the *para* or *meta* positions (e.g., **9x–z** and **10l** and **10m**) substantially reduced cytotoxicity. This may be due to compacting or “folding” of these chains in the minor groove leading to a reduced fit. Compounds with cyclic C2-substituents such as 4-(4-methyl)piperazinyl (**9a'**) and 4-morpholinyl (**9b'**) are exceptions with very low IC₅₀ values. One possible explanation is that entropic costs are minimized with cyclic C2-substituents. With the C2-pyridinyl compounds **14d–e**, the position of the nitrogen in the ring does not appear to significantly affect cytotoxicity. Likewise, exchange of the heteroatom between 2-benzofuranyl (**14g**) and 2-benzothiophenyl (**14h**) analogues does not enhance activity. However, the presence of a *N*-methyl group in the 4-pyrazolyl conjugates (**14b–c**)

improves cytotoxicity. Finally, carboxylic acid groups as in **9t** and **10i** completely deplete cytotoxicity, possibly due to repulsion between the negative charges encountered in the DNA and the substituents in these specific PBDs.

Insertion of a naphthyl substituent at the C2-position dramatically increases both the DNA binding affinity and cytotoxicity of PBD monomers, as can be seen from the ΔT_m and IC_{50} values for the C2-(2-naphthyl)-substituted compound **13a** ($IC_{50} = 0.5724 \mu M$, $\Delta T_m = 15.8^\circ C$). On the basis of the decreased cytotoxicity of the C2-(1-naphthyl) analogue **13d**, it would appear that the best position for joining

Table 4. Cytotoxicity Data for the C2-Aryl PBD C11-(Sodium Bisulfite) Adducts



Code	Compound R ₁	NCI Screen (μM) ^a			K562 IC_{50} ^b (μM)	
		GI ₅₀	TGI	LC ₅₀	N10-C11 Imine	N10-C11 bisulfite
28a		0.054	0.43	5.75	0.0025	0.0165
28b		0.008	0.05	0.95	0.0478	0.0700
28c		0.005	0.04	10.0	0.0016	0.0163
28d		0.005	0.07	0.63	0.0004	0.0071
28e		0.002	0.02	2.57	0.0454	0.0018
28f		0.0002	0.004	0.35	0.0014	0.0013

^a NCI 60 cell-line panel. Figures correspond to the mean values (MG-MID) calculated from the 60 individual cell lines (see Supporting Information). ^b K562 human chronic myeloid leukemia cell line (96 h incubation, see Experimental Section).

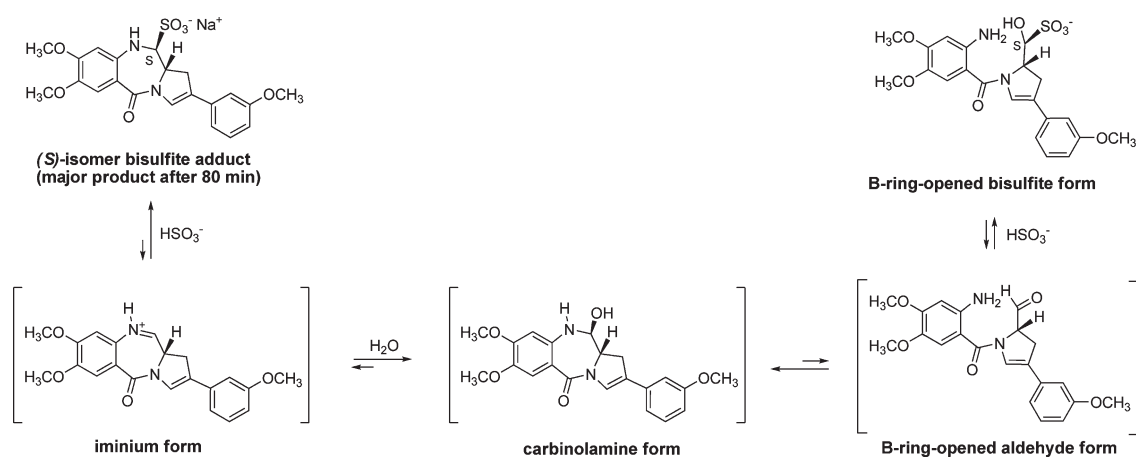


Figure 3. Possible interconvertible forms present in an aqueous solution of **28d** based on NMR. (Note: Structures in brackets are proposed based on sequential addition/elimination mechanisms and have not been observed by NMR.)

fused ring systems to the C2-position of a PBD is furthest from the bridge carbons (i.e., the 2-position using the naphthalene ring numbering system). In support of this, NMR studies have revealed that for the C2-(2-naphthyl) system, the 2-naphthyl ring lies along the minor groove extending the isohelical shape created by the A-, B-, and C-rings of the PBD skeleton.⁴³ For the C2-(1-naphthyl) configuration, the naphthyl ring can take up two possible conformations, one in which it clashes with the floor of the minor groove or another in which it points out of the groove, neither of which are conducive to a good overall fit of the PBD molecule. This concept is also supported by the decreased cytotoxicity of the 4-dibenzothiophenyl (**15a**), 4-dibenzofuranyl (**15b**) and 1-thianthrenyl (**15c**) analogues.

The C2-heteroaryl sublibrary contained the most active compounds, with the C2-quinolynyl-substituted analogues **14k** and **14l** providing greater DNA stabilization than the corresponding C2-(2-naphthyl) analogue **13a** (Table 2). The C2-(6-quinolynyl) PBD (**14l**) has the highest ΔT_m value of all the compounds examined ($\Delta T_m = 20.5^\circ C$), which is also reflected in its high cytotoxicity ($IC_{50} = 1.4 \text{ nM}$ in K562). Modeling studies with four 1:1 (ligand/DNA) complexes with the 9-mer DNA duplex sequence d(5'-CGCA-GACGC-3').d(5'-GCGTCTGCG-3') (Figure 4A) provided estimates of differences in relative stabilization energies. These were calculated relative to the value for the 9-mer DNA adduct with compound **8**:

$$\mathbf{8}-(9\text{-mer DNA}) : 0.0 \text{ kcal mol}^{-1}$$

$$\mathbf{12b}-(9\text{-mer DNA}) : +18.2 \text{ kcal mol}^{-1}$$

$$\mathbf{13a}-(9\text{-mer DNA}) : -0.4 \text{ kcal mol}^{-1}$$

$$\mathbf{14l}-(9\text{-mer DNA}) : -2.2 \text{ kcal mol}^{-1}$$

These values are in good qualitative agreement with the rank order of ΔT_m values and show that the C2-quinolynyl substituent in **14l** is the best in energetic terms. The outstandingly higher energy of the dimethyl adduct (**12b**) is a consequence of the reduction in nonbonded interactions between the DNA minor groove walls and the phenyl group as a result of steric clashes involving the methyl groups. Figure 4A shows that the C2-substituent is forced out of the groove as a consequence. It is also notable that compound

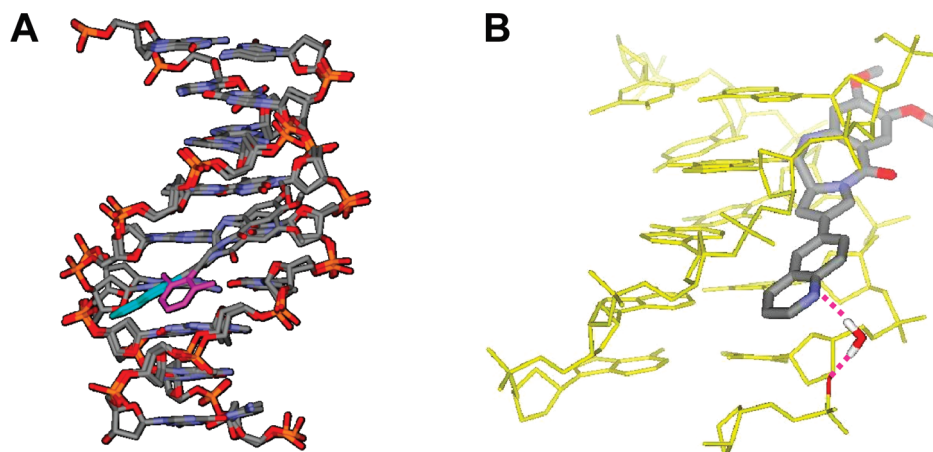


Figure 4. (A) Overlay of the final minimized simulated structures of the covalent complexes between the duplex DNA sequence $d(5'-CGCAGACGC-3')$. $d(5'-GCGTCTGCG-3')$ and compounds **12b** and **14l**. The 2,6-dimethylphenyl group in the former is colored magenta and the quinolinylnyl ring in the latter is cyan. (B) Snapshot of a model of part of the **(14l)₂**-DNA adduct [$d(5'-AATCTTTAAAGATT-3')_2$] with the C2-quinolinylnyl substituent of **14l** in the “inward conformation”. Conformational search (MacroModel, version 9.6) predicted indirect H₂O-bridged H-bonding interactions between the C2-quinolinylnyl nitrogen atom and backbone atoms of the noncovalently modified DNA strand. Direct H-bonding interactions between the nitrogen atom and DNA bases were not predicted from these studies.

12b has correspondingly poor cytotoxicity compared to other compounds in the series, confirming that biological potency is related to minor groove binding.

The improved energy of **14l** relative to the 2-naphthyl derivative (**13a**) is due, at least in part, to the polarization induced by the ring nitrogen atom which enhances the electrostatic contribution to the overall energy. Another possible explanation relates to the hydrogen bonding potential of the ring nitrogen in **14l**. We initially assumed that the nitrogen atom in the quinolinylnyl ring may interact with DNA bases via hydrogen bonding interactions (H-bonds). However, initial molecular modeling experiments failed to reveal any direct H-bonds between **14l** and DNA, although it was established that the quinolinylnyl ring of **14l** could adopt two different conformations in the minor groove both potentially conducive to bonding. In one case, it is aligned along the minor groove (the “inward conformation”, see Figure 4B) and in the other the ring is protruding slightly from the groove (the “outward conformation”).⁴³ Preliminary energy minimization experiments using implicit solvent were carried out with both conformations and 16 different 8-mer DNA duplex sequences (i.e., $d(5'-TAXXGATT-3')$. $d(5'-AATCYYTA-3')$ where X = G, A, T or C) in order to account for all possible permutations for the base pairs in close proximity to the naphthyl and quinolinylnyl rings. The preliminary results showed that, as anticipated, the total energies for the two different types of conformations across all 16 adducts had an average difference of 24.5 kcal mol⁻¹ in favor of the inward conformation. This result supports recent NMR studies on a **(13a)₂**-DNA adduct which demonstrated that the C2-naphthyl ring of **13a** lies along the hydrophobic floor of the minor groove.⁴³ However, no discrete H-bonds were observed in any of the 16 models, and so we next performed conformational searches on a selected 14-mer **(14l)₂**-DNA adduct [$d(5'-AATCTTTAAAGATT-3')_2$]⁴³ in the inward conformation in the presence of water molecules using MacroModel (version 9.6) (Figure 4B). The results of this computational analysis suggested that **14l** in the “inward conformation” can interact with DNA through H-bonds involving the ring nitrogen of the C2-quinolinylnyl substituent, water molecules, and the backbone atoms of the noncovalently modified DNA strand (Figure 4B). These additional interactions could further stabilize the DNA

duplex upon adduct formation and may explain the higher ΔT_m value of this compound compared to **13a**.

C2-Styryl PBD Imines. To further explore the SAR of C2-aryl PBDs, we designed a set of C2-styryl analogues (Table 3) in which the sp² C2-carbon is distanced further from the aryl substituent by a conjugated double bond. The cytotoxicity data for **16a–e** show that this arrangement still enhances potency, not only compared to C2-aryl analogues but also to the C2-vinyl compound **32**. The unsubstituted styryl derivative **16a** and the 4-fluoro-substituted **16c** were highly cytotoxic in both the NCI and K562 cell lines. The (4-CH₃)-substituted styryl **16b** gave an intermediate ΔT_m value of 14.0 °C, which ranks between the average ΔT_m for the C2-phenyl PBDs (~10.0 °C) and the ~20.0 °C observed for the C2-quinolinylnyl PBDs.

C2-Aryl PBD C11-(Sodium Bisulfite) Adducts. All C11-bisulfite library members (**28a–f**) are freely soluble in water as opposed to their N10–C11 imine precursors. However, with the exception of the C2-naphthyl **28e** (more active) and C2-quinolinylnyl **28f** (equipotent) adducts (Table 4), all the remaining C11-(sodium bisulfite) adducts were less cytotoxic in both the NCI panel and the K562 leukemia cell line in comparison to the equivalent parent PBD N10–C11 imines from which they derive. To verify that DNA interaction was occurring in a similar manner to the parent N10–C11 imines, MS-MALDI experiments (see Supporting Information) were carried out to confirm covalent interaction and identical stoichiometry after reaction of both the PBD imine **13a** and its C11-bisulfite derivative (**28e**) with a 14-mer DNA duplex. This provides further evidence that PBD C11-bisulfites are acting as “prodrugs” in solution to generate a low but steady concentration of the equivalent PBD imine species, thus leading to a slower reaction with DNA compared to the parent PBD imines.⁸ As the imine species react with DNA, albeit slowly, the equilibrium presumably adjusts until eventually all C11-bisulfite is consumed. This also explains the higher IC₅₀ values compared to their PBD imine counterparts.

In Vivo Studies. Evaluation of 14l in a HCT-116 Human Tumour Xenograft Model. On the basis of the unusually high DNA-binding affinity of the C2-(6-quinolinylnyl) PBD monomer **14l**, it was progressed into an in vivo human tumor

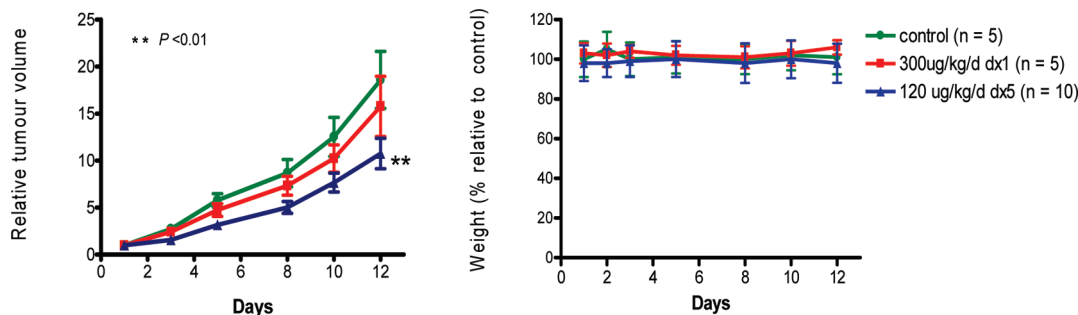


Figure 5. Left: **14I** inhibits the growth of HCT-116 tumors in nude mice. Randomized HCT-116 tumor-bearing mice were injected iv with either a single bolus injection of 300 µg/kg or daily 120 µg/kg injections for 5 days. The change in tumor volume at each time point was determined for each animal (as tumor volume relative to tumor volume at the beginning of treatment – day 1). The line graphs show the mean relative tumor volumes for the animals in each treatment group. Asterisks depict the statistical significance of the differences between the control group and each of the **14I** treatment groups (using Student's *t*-test). Right: Animal weights are provided as percentage change relative to animal weights at day 1. Error bars in both panels represent standard error.

xenograft mouse model inoculated with the HCT-116 cell line, a widely used xenograft model. Both irinotecan and capecitabine have been reported to induce significant growth delays and regression in this model.^{50,51} Two schedules of administration were evaluated: a single iv injection of 300 µg/kg, and five consecutive daily iv injections of 120 µg/kg (1 cycle from day 1 to day 5). The results are statistically significant (Student's *t*-test) and demonstrate not only the ability of **14I** to delay tumor growth in this model but also the prolonged benefit of treatment ($P_{\text{value}} < 0.01$) (Figure 5, left). Crucially, at these doses and different schedules of administration, there was no apparent toxicity as judged by a lack of significant adverse effects or reduction of animal weights throughout the treatment (Figure 5, right).

Conclusions

Novel synthetic methodologies have been applied to advance understanding of the SAR profile of PBD monomers. An 80-member library containing a wide variety of substituents at the C2-position of the PBD skeleton has been successfully prepared using three different approaches involving the palladium-catalyzed cross-coupling of enol-triflate substrates. The cytotoxicity data demonstrated a wide range of activities across the library. In the simple C2-phenyl-substituted series, activity does not appear to depend significantly on the position of substituents in the benzene ring, although there is limited evidence that electron-withdrawing substituents are favorable for optimal activity. However, there is clear evidence that fused aromatic ring systems (e.g., 2-naphthyl) markedly improve both DNA binding and cytotoxicity, although for optimal activity the point of attachment of the fused ring system to the C2-position of the PBD must not be immediately adjacent to the bridge atoms of the fused ring system to avoid clashes with the walls of the host DNA minor groove. Moreover, insertion of heteroatoms into a C2-naphthyl moiety can substantially enhance both cytotoxicity and DNA-binding affinity (i.e., the 3- and 6-quinolinyl analogues). Interestingly, C2-styryl compounds were found to be significantly more cytotoxic in the K562 cell line compared to other C2-substituted sub-library members. Finally, we have shown that formation of C11S-(sodium bisulfite) adducts dramatically improves the water solubility of C2-aryl PBD-imines, although surprisingly they are less potent than their PBD-imine counterparts. This may be due to these adducts acting as “prodrugs”, with slow hydrolysis resulting in release of the DNA-reactive N10–C11 imine species.⁸

Overall, this study has provided a substantial body of SAR data (Figure 2) relating to C2-substituted PBD monomers, demonstrating that some substituents (e.g., C2-quinolinyl) can enhance both cytotoxicity and DNA-binding affinity to a similar level of potency as that observed for PBD dimers which can form covalent interstrand cross-links between DNA strands. Finally, the ability of **14I** to delay tumor growth at doses not associated with significant weight loss or other adverse effects in the HCT-116 colon cancer xenograft model suggests that C2-aryl PBD monomers may have potential in the treatment of human disease.

Experimental Section

Chemistry. General Synthetic Methods. Optical rotations were measured on an ADP 220 polarimeter (Bellingham Stanley Ltd.) and concentrations (*c*) are given in g/100 mL. Melting points were measured using a digital melting point apparatus (Electrothermal). IR spectra were recorded on a Perkin-Elmer Spectrum 1000 FT IR spectrometer. ¹H and ¹³C NMR spectra were acquired at 300 K using a Bruker Avance NMR spectrometer at 400 and 100 MHz, respectively, unless stated otherwise. Chemical shifts are reported relative to TMS ($\delta = 0.0$ ppm), and signals are designated as s (singlet), br s (broad singlet), d (doublet), t (triplet), q (quadruplet), qu (quintuplet), h (heptuplet), dt (double triplet), dd (doublet of doublets), ddd (double doublet of doublets), or m (multiplet), with coupling constants given in Hertz (Hz). A pro-PBD numbering system has been used for carbon and proton assignments for synthetic intermediates (i.e., based on the final tricyclic PBD ring system). Mass spectroscopy data were collected using a Waters Micromass ZQ instrument coupled to a Waters 2695 HPLC with a Waters 2996 PDA. Waters Micromass ZQ parameters used were: capillary, 3.38 kV; cone, 35 V; extractor, 3.0 V; source temperature, 100 °C; desolvation temperature, 200 °C; cone flow rate, 50 L/h; desolvation flow rate, 250 L/h. High-resolution mass spectroscopy data were recorded on a Waters Micromass QTOF Global in positive W-mode using metal-coated borosilicate glass tips to introduce samples into the instrument. Thin-layer chromatography (TLC) was performed on silica gel aluminum plates (Merck 60, F₂₅₄), and flash chromatography utilized silica gel (Merck 60, 230–400 mesh ASTM). All chemicals and anhydrous solvents were purchased from Sigma-Aldrich. Compounds **8–16** (Tables 1 and 3) were synthesized according to previously described methodology.³⁵ The novel PBD-imine C2-quinolinyl (**14k–l**) and C2-styryl (**16a–e**) compounds reported here were synthesized as part of this study and purified accordingly. All compounds used in the biophysical and biological evaluations were >95% pure as determined by previously described HPLC methodology.³⁵ Analytical data for these compounds are collected in Supporting Information.

Synthesis of the Fully Saturated C-Ring C2-Aryl PBD Imine (27). (S)-Benzyl 2-((*tert*-Butyldimethylsilyloxy)methyl)-4-oxopyrrolidine-1-carboxylate (**18**). TEMPO (0.1 g, 0.68 mmol, 0.1 equiv) and BAIB (2.43 g, 7.53 mmol, 1.1 equiv) were added to a solution of Cbz-protected amine alcohol **17**³⁹ (2.5 g, 6.84 mmol, 1.0 equiv) in CH₂Cl₂ (50 mL), and the mixture stirred for 2 h when TLC (EtOAc/hexane 1:1) indicated complete consumption of starting material. The reaction mixture was diluted with CH₂Cl₂ (100 mL) and washed with saturated aqueous Na₂S₂O₃ (60 mL). The aqueous layer was extracted with CH₂Cl₂ (2 × 50 mL), and the combined organic layer was washed with brine (50 mL) and dried over MgSO₄. Removal of excess solvent under reduced pressure afforded a solid that was purified by flash column chromatography (EtOAc/hexane 3:7 v/v) to afford **18** (1.2 g, 48%). ¹H NMR (CDCl₃) rotamers: δ -0.02–0.06 (m, 6 H, Si(CH₃)₂), 0.83 (s, 9 H, C(CH₃)₃), 2.45 (d, 1 H, *J* = 17.9 Hz, H1), 2.67 (m, 1 H, H1), 3.56 (d, 1 H, *J* = 10.3 Hz, H3), 3.74 (d, 1 H, *J* = 18.4 Hz, H11), 3.72–4.07 (m, 2 H, H3 and H11), 4.39–4.48 (m, 1 H, H11a), 5.18 (s, 2 H, CH₂-CBz), 7.33–7.39 (m, 5 H, Ar-CBz). ¹³C NMR (CDCl₃): δ 209.9 (C2), 154.4 (NC=O), 136.4 (Ar-CBz), 127.9–128.5 (Ar-CBz), 67.3 (C11), 64.9 (CH₂-CBz), 55.8 (C11a), 53.7 (C3), 40.1 (C1), 25.7 (C(CH₃)₃), 18.0 (Cquat), -5.8 (SiCH₃)₂.

(S)-Benzyl 2-((*tert*-Butyldimethylsilyloxy)methyl)-4-(trifluoromethylsulfonyloxy)-2,5-dihydro-1*H*-pyrrole-1-carboxylate (**19**). A cold (-78 °C) solution of ketone **18** (800 mg, 2.20 mmol, 1.0 equiv) in THF (20 mL) was added slowly to a stirred solution of sodium bis(trimethylsilyl)amide (2.4 mL, 2.4 mmol, 1.1 equiv) in THF (20 mL) at -78 °C. After 1 h, a cold (-20 °C) solution of *N,N*-bis(trifluoromethanesulfonyl)anilide (0.96 g, 2.4 mmol, 1.1 equiv) in THF (20 mL) was cannulated into the flask and the reaction mixture was allowed to warm slowly to room temperature. After 4 h, TLC (EtOAc/hexane 3:7 v/v) indicated complete consumption of starting material. The excess solvent was then removed under reduced pressure, and the residue was subjected to flash chromatography purification (EtOAc/hexane 1:9 v/v) to afford the enol-triflate **19** (1.0 g, 2.02 mmol, 91%). [α]_D²¹ = -0.25° (*c* = 0.18, CHCl₃). IR (film, ν_{max}/cm⁻¹): 1716, 1429, 1328, 1219, 1140, 837. ¹H NMR (CDCl₃) rotamers: δ -0.04–0.02 (m, 6 H, Si(CH₃)₂), 0.86 (s, 9 H, C(CH₃)₃), 3.66–3.88 (m, 2 H, H11), 4.20–4.41 (m, 2 H, H3), 4.61–4.69 (m, 1 H, H11a), 5.18 (s, 2 H, CH₂-CBz), 5.74 (d, 1 H, *J* = 8.4 Hz, H1), 7.31–7.40 (m, 5 H, Ar-CBz). ¹³C NMR (CDCl₃) rotamers: δ 154.1 (NCO-CBz), 143.5 (C2), 139.2 (Ar-CBz), 128.1–128.6 (Ar-CBz), 115.2 (C1), 118.5 (q, *J* = 256 Hz from ¹³C¹⁹F₃ coupling, CF₃), 67.3 (CH₂-CBz), 63.6 (C11), 62.6 (C11a), 50.1 (C3), 25.7 (C(CH₃)₃), 18.1 (Cquat), -5.6 (SiCH₃)₂.

(S)-Benzyl 2-((*tert*-Butyldimethylsilyloxy)methyl)-4-(4-methoxyphenyl)-2,5-dihydro-1*H*-pyrrole-1-carboxylate (**20**). 4-Methoxyphenylboronic acid (0.37 g, 2.42 mmol, 1.0 equiv) and Pd(PPh₃)₄ (0.03 g, 0.024 mmol, 0.01 equiv) were added to a solution of enol-triflate **19** (1.2 g, 2.42 mmol, 1.0 equiv) in toluene (50 mL) at room temperature. After stirring for 5 min, a 2.0 M aqueous solution of Na₂CO₃ was added to the mixture. The reaction mixture was stirred at room temperature for 36 h when TLC (EtOAc/hexane 3:7 v/v) indicated complete consumption of starting material. Excess solvent was removed, and the residue was dissolved in EtOAc (50 mL), washed with water (50 mL) and brine (50 mL), and dried over MgSO₄. Filtration and evaporation of solvent afforded the crude product which was purified by flash column chromatography (hexane/EtOAc 1:9 v/v) to afford **20** as a white glass (0.5 g, 45%). [α]_D²² = -0.32° (*c* = 0.20, CHCl₃). IR (film, ν_{max}/cm⁻¹): 1710, 1609, 1515, 1416, 1257, 1112, 836. ¹H NMR (CDCl₃) rotamers: δ 0.0–0.07 (m, 6 H, Si(CH₃)₂), 0.89 (s, 9 H, C(CH₃)₃), 3.62–4.04 (m, 2 H, H11), 3.82 (s, 3 H, 4'-OCH₃), 4.45–4.67 (m, 2 H, H3), 4.63–4.79 (m, 1 H, H11a), 5.19–5.29 (m, 2 H, CH₂-CBz), 6.09 (d, 1 H, *J* = 4.4 Hz, H1), 6.89–6.93 (m, 2 H, H3' and H5'), 7.30–7.46 (m, 7 H, Ar-CBz, H2' and H6'). ¹³C NMR (CDCl₃) rotamers: δ 159.5 (C4'), 154.5 (NCO-CBz), 136.6–137.1

(C1' and Ar-CBz), 125.9–128.5 (C2', C6', and Ar-CBz), 120.5 (C1), 114.0 (C3' and C5'), 67.1 (CH₂-CBz), 66.3 (C11a), 64.9 (C11), 54.6 (C3), 55.3 (4'-OCH₃), 25.8 (C(CH₃)₃), 18.2 (Cquat), -5.4 (SiCH₃)₂.

(2*S*,4*R*)-2-((*tert*-Butyldimethylsilyloxy)methyl)-4-(4-methoxyphenyl)pyrrolidine (**21**). A catalytic amount of 10% palladium on carbon (50 mg) was added to a solution of Cbz-protected compound **20** (0.5 g, 1.10 mmol) in absolute EtOH (30 mL). The reaction mixture was hydrogenated under a H₂ balloon for 12 h. When reaction was complete as indicated by TLC (EtOAc/hexane 15:85 v/v), the reaction mixture was filtered through celite and excess solvent removed under reduced pressure to afford the amine **21** (0.36 g, 99%), which was used in the subsequent reaction without further purification. MS (ESI⁺) *m/z* (relative intensity): 322.1 ([*M* + H]⁺, 8%), 364.2 ([*M* + CH₃CN + H]⁺, 100%).

(2*S*,4*R*)-2-((*tert*-Butyldimethylsilyloxy)methyl)-4-(4-methoxyphenyl)pyrrolidin-1-yl(4,5-dimethoxy-2-nitrophenyl)methanone (**22**). EDCI (0.26 g, 1.35 mmol, 1.2 equiv) was added to a stirred solution of the carboxylic acid (0.31 g, 1.35 mol, 1.2 equiv) in anhydrous CH₂Cl₂ (30 mL) under a nitrogen atmosphere at 0 °C. After stirring for 10 min, the mixture was treated with HOBt (0.18 g, 1.35 mmol, 1.2 equiv) and a few drops of DMF, and the resulting mixture allowed to warm to room temperature and stirred for 2 h. The mixture was again cooled to 0 °C and treated dropwise with a solution of amine **21** (0.36 g, 1.12 mmol, 1.0 equiv) in anhydrous CH₂Cl₂ (10 mL). When reaction was complete, as indicated by TLC (EtOAc/hexane 1:1 v/v), the reaction mixture was diluted with CH₂Cl₂ (30 mL), washed with 1 N HCl (20 mL), saturated aqueous NaHCO₃ (20 mL), and brine (20 mL), and then dried (MgSO₄), filtered, and evaporated in vacuo. The title compound **22** was purified by flash column chromatography (EtOAc/hexane 3:7 v/v) to provide a brown solid (0.44 g, 74%). [α]_D²² = -0.26° (*c* = 0.20, CHCl₃). IR (film, ν_{max}/cm⁻¹): 1644, 1580, 1516, 1429, 1337, 1277. ¹H NMR (CDCl₃): δ 0.13 (s, 6 H, Si(CH₃)₂), 0.95 (s, 9 H, C(CH₃)₃), 2.26–2.48 (m, 2 H, H1), 3.16–3.40 (m, 3 H, H2 and H3), 3.76 (s, 3 H, 4'-OCH₃), 3.94 (s, 6 H, 7,8-OCH₃), 3.90 (br s, 1 H, H11), 4.25 (br s, 1 H, H11), 4.47 (br s, 1 H, H11a), 6.77 (s, 1 H, H6), 6.80 (d, 2 H, *J* = 8.6 Hz, H3' and H5'), 7.11 (d, 2 H, *J* = 8.6 Hz, H2' and H6'), 7.67 (s, 1 H, H9). ¹³C NMR (CDCl₃) rotamers: δ 166.5 (C5), 158.6 (C4'), 154.1 (C7), 148.8 (C8), 137.6 (C9a), 131.9 (C1'), 128.2 (C5a), 128.1 (C2' and C6'), 114.0 (C3' and C5'), 109.2 (C6), 107.2 (C9), 62.7 (C11), 58.8 (C11a), 57.3 (C3), 56.6, 56.5 (7-OCH₃ and 8-OCH₃), 55.3 (4'-OCH₃), 43.2 (C2), 34.5 (C1), 25.8 (C(CH₃)₃), 18.2 (Cquat), -5.5 (SiCH₃)₂. MS (ESI⁺) *m/z* (relative intensity): 531.3 ([*M* + H]⁺, 100%).

(2-Amino-4,5-dimethoxyphenyl)((2*S*,4*R*)-2-((*tert*-butyldimethylsilyloxy)methyl)-4-(4-methoxyphenyl)pyrrolidin-1-yl)methanone (**23**). A catalytic amount of 10% palladium on carbon (25 mg) was added to a solution of **22** (0.25 g, 0.47 mmol) in absolute EtOH (30 mL). The reaction mixture was hydrogenated under a H₂ balloon for 12 h, and when reaction was complete as indicated by TLC (EtOAc-hexane 1:1 v/v), the reaction mixture was filtered through celite and excess solvent removed under reduced pressure to afford the amine **23** which was used in the subsequent reaction without further purification (170 mg, 72%). [α]_D¹⁸ = -0.10° (*c* = 0.22, CHCl₃). MS (ESI⁺) *m/z* (relative intensity): 501.3 ([*M* + H]⁺, 100%) (see Supporting Information for IR and NMR data).

Allyl 2-((2*S*,4*R*)-2-((*tert*-Butyldimethylsilyloxy)methyl)-4-(4-methoxyphenyl)pyrrolidine-1-carbonyl)-4,5-dimethoxyphenylcarbamate (**24**). Pyridine (0.11 mL, 1.36 mmol, 2.2 equiv) was added to a stirred solution of the amine **23** (0.31 g, 0.62 mmol, 1.0 equiv) in CH₂Cl₂ (20 mL) at 0 °C under a N₂ atmosphere. The cooled mixture was then treated dropwise with a solution of allyl chloroformate (0.10 mL, 0.93 mmol, 1.5 equiv) in CH₂Cl₂ (10 mL). After 6 h stirring at room temperature, the mixture was diluted with CH₂Cl₂ (30 mL), washed with 1 N HCl (20 mL), water (20 mL) and brine (20 mL), and then dried (MgSO₄),

filtered, and evaporated in vacuo. The crude residue was purified by flash chromatography (EtOAc/hexane 2:8 v/v) to afford the alloc-protected product **24** as a pale orange solid (0.30 g, 82%). MS (ESI⁺) *m/z* (relative intensity): 585.3 ([*M* + H]⁺, 100%).

Allyl 2-(2*S*,4*R*)-2-(Hydroxymethyl)-4-(4-methoxyphenyl)pyrrolidine-1-carbonyl)-4,5-dimethoxyphenylcarbamate (25). To a solution of **24** (0.3 g, 0.51 mmol, 1.0 equiv) in THF (30 mL) at 0 °C under a N₂ atmosphere, a solution of TBAF (0.61 mL of a 1 M solution in THF, 0.61 mmol, 1.2 equiv) was added. The mixture was allowed to warm to room temperature and stirring continued for a further 3 h when TLC (EtOAc/hexane 1:1 v/v) revealed complete consumption of starting material. The excess solvent was removed, the residue dissolved in EtOAc (30 mL), and the solution washed with saturated aqueous NH₄Cl (10 mL) and brine (10 mL), and then dried (MgSO₄). Evaporation of the solvent in vacuo afforded the crude product that was purified by flash column chromatography (EtOAc/hexane 1:1 v/v) to afford **25** as a white solid (0.23 g, 96%). [α]_D²⁰ = 0.17° (*c* = 0.19, CHCl₃). MS (ESI⁺) *m/z* (relative intensity): 471.2 ([*M* + H]⁺, 70%). (See Supporting Information for IR and NMR data).

(2*R*,11*S*,11*aS*)-Allyl 11-Hydroxy-7,8-dimethoxy-2-(4-methoxyphenyl)-5-oxo-2,3,11,11a-tetrahydro-1*H*pyrrolo[2,1-*c*][1,4]benzodiazepine-10(5*H*)-carboxylate (26). BAIB (0.17 g, 0.54 mmol, 1.1 equiv) and TEMPO (0.01 g, 0.05 mmol, 0.1 equiv) were added to a solution of the alcohol **25** (0.23 g, 0.49 mmol, 1.0 equiv) in CH₂Cl₂ (10 mL), and the mixture stirred at room temperature for 5 h. When reaction was complete as indicated by TLC (EtOAc), the mixture was diluted with CH₂Cl₂ (20 mL) and washed with saturated Na₂S₂O₃ (10 mL). The aqueous layer was extracted with CH₂Cl₂ (2 × 30 mL) and the combined organic layer washed with brine (20 mL) and dried (MgSO₄). Evaporation in vacuo afforded a solid that was purified by flash column chromatography (EtOAc/hexane 1:1 v/v) to afford **26** as a white solid (0.15 g, 65%). [α]_D¹⁸ = +0.40° (*c* = 0.16, CHCl₃). IR (film, ν_{\max} /cm⁻¹): 3351, 1709, 1605, 1516, 756. ¹H NMR (CDCl₃): δ 2.11–2.17 (m, 1 H, H1), 2.72 (qu, 1 H, *J* = 7.4 Hz, H1), 3.27–3.36 (m, 2 H, H2 and H3), 3.62–3.69 (m, 2 H, H11a and OH), 3.80 (s, 3 H, 4'-OCH₃), 3.87 (s, 3 H, 7-OCH₃), 3.94 (s, 3 H, 8-OCH₃), 4.50 (br s, 1 H, CH₂-Alloc), 4.55 (dd, 1 H, *J* = 7.4, 13.9 Hz, H3), 4.69 (dd, 1 H, *J* = 6.6, 13.9 Hz, CH₂-Alloc), 5.15 (d, 2 H, *J* = 11.8 Hz, CH=CH₂-Alloc), 5.73 (br s, 1 H, H11), 5.81 (br s, 1 H, CH=CH₂-Alloc), 6.69 (s, 1 H, H9), 6.88 (d, 2 H, *J* = 10.1 Hz, H3' and H5'), 7.18 (d, 2 H, *J* = 10.1 Hz, H2' and H6'), 7.27 (s, 1 H, H6). ¹³C NMR (CDCl₃): δ 167.3 (C5), 158.7 (C4'), 156.0 (C=O-Alloc), 150.8 (C9a), 148.4 (C8), 131.8 (C7 and C1'), 128.5 (CH=CH₂-Alloc), 128.0 (C2' and C6'), 124.8 (C5a), 118.1 (CH=CH₂-Alloc), 114.2 (C3' and C5'), 112.3 (C9), 110.8 (C6), 88.0 (C11), 66.8 (CH₂-Alloc), 59.7 (C11a), 56.1 (7,8-OCH₃), 55.3 (4'-OCH₃), 51.8 (C3), 42.1 (C2), 38.4 (C1). MS (ESI⁺) *m/z* (relative intensity): 469.2 ([*M* + H]⁺, 100%).

(2*R*,11*aS*)-7,8-Dimethoxy-2-(4-methoxyphenyl)-2,3-dihydro-1*H*-pyrrolo[2,1-*c*][1,4]benzodiazepin-5(11*aH*)-one (27). A catalytic amount of tetrakis(triphenylphosphine)palladium (3.7 mg, 3.0 μ mol, 0.01 equiv) was added to a stirred solution of the alloc-protected carbinolamine **26** (150 mg, 0.32 mmol, 1.0 equiv) and pyrrolidine (30 μ L, 0.35 mmol, 1.1 equiv) in CH₂Cl₂ (20 mL). After stirring for 30 min at room temperature under a N₂ atmosphere, TLC (EtOAc) indicated complete consumption of starting material. The solvent was evaporated in vacuo and the crude product purified by flash chromatography (EtOAc) to afford **27** as a colorless glass which was repeatedly evaporated from CHCl₃ in vacuo to provide the imine **27** as a light-yellow solid (68 mg, 58%). [α]_D¹⁹ = +1.76° (*c* = 0.26, CHCl₃). IR (film, ν_{\max} /cm⁻¹): 1603, 1514, 1434, 1251, 1034, 758. ¹H NMR (CDCl₃): δ 2.36–2.45 (m, 1 H, H1 β), 2.74–2.83 (m, 1 H, H1 α), 3.39–3.49 (m, 1 H, H2), 3.61 (dd, 1 H, *J* = 9.2, 12.0 Hz, H3 β), 3.80 (s, 3 H, 4'-OCH₃), 3.92 (s, 3 H, 7-OCH₃), 3.96 (s, 3 H, 8-OCH₃), 3.85–4.00 (m, 1 H, H11a), 4.34 (dd, 1 H, *J* = 7.5, 12.1

Hz, H3 α), 6.81 (s, 1 H, H9), 6.89 (d, 2 H, *J* = 8.6 Hz, H3' and H5'), 7.20 (d, 2 H, *J* = 8.6 Hz, H2' and H6'), 7.54 (s, 1 H, H6), 7.64 (d, 1 H, *J* = 4.1 Hz, H11). ¹³C NMR (CDCl₃): δ 164.8 (C5), 162.7 (C11), 158.8 (C4'), 151.5 (C8), 147.7 (C7), 140.8 (C9a), 131.5 (C1'), 128.0 (C2' and C6'), 119.5 (C5a), 114.1 (C3' and C5'), 111.6 (C6), 109.7 (C9), 56.1 (7,8-OCH₃), 55.3 (4'-OCH₃), 54.0 (C11a), 52.6 (C3), 41.4 (C2), 37.7 (C1). MS (ESI⁺) *m/z* (relative intensity): 365.3 ([*M* - H]⁻, 40%).

General Methodology for the Synthesis of C2-Aryl PBD-C11-(Sodium Bisulfite) Adducts. A solution of C2-aryl PBD-imine (0.06 mmol, 1.0 equiv) in CH₂Cl₂ (1.0 mL) was added to a freshly prepared aqueous solution of NaHSO₃ (1.0 mL; 0.06 mmol, 1.1 equiv) in a test tube, and the two-phase system was vigorously stirred for 4 h at room temperature. The work-up involved washing with CH₂Cl₂ (3 × 1 mL) using a phase-separator cartridge pre-conditioned with CH₂Cl₂ (1.0 mL). The organic layers were removed, and the remaining aqueous solution lyophilized to afford the bisulfite adducts **28a–f** (yield and analytical data for **28a** are provided below; see Supporting Information for **28b–f**) [NOTE 1: The purity of the C2-aryl bisulfite adducts ranged from 86% to 97% as determined by previously described HPLC methodology.³⁵ However, analysis of LC-MS traces relating to the additional UV-detected peaks gave molecular ions ([*M* + H]⁺) for the corresponding PBD imines. For example, LC-MS profile [UV-peak (min); (ESI⁺) *m/z*, relative intensity] for compound **28d** (two peaks): 7.02 min; 447.48 (C11-bisulfite: [*M* - Na + H]⁺, 100%) and 7.23 min; 365.59 (N10-C11 imine: [*M* - SO₃⁻Na⁺ + H]⁺, 30%), and 383.56 (C11-carbinolamine ([*M* + H₂O + H]⁺, 100%). The same sample showed only the C11(S)-(sodium bisulfite) species by ¹H-NMR (D₂O and *d*₆-DMSO). Taken together with the ¹H-NMR data, these results indicate an equilibrium between the imine and bisulfite species. It is probable that the low pH of the HPLC mobile phase displaced the equilibrium towards the imine form, which might be expected to be present in non-detectable amounts in the neutral solutions employed for NMR analyses]. A more efficient conversion to C11S-(sodium bisulfite) adducts can be achieved by vigorously vortexing the emulsion as fully described in the time-course ¹H-NMR experiments in Supporting Information.

Representative Compound. (11*S*,11*aS*)-7,8-Dimethoxy-2-(phenyl)-5-oxo-5,10,11,11a-tetrahydro-1*H*-pyrrolo[2,1-*c*][1,4]benzodiazepine-11-sulfonic Acid Sodium Salt (28a). Yield 79%, 8 mg. ¹H NMR (DMSO): δ 3.26 (ddd, 1 H, *J* = 2.04, 10.23, 16.85 Hz, H1 α), 3.52 (dd, 1 H, *J* = 2.51, 17.10 Hz, H1 β), 3.71 (s, 3 H, 7-OCH₃), 3.77 (s, 3 H, 8-OCH₃), 3.96 (d, 1 H, *J* = 10.36 Hz, H11), 4.32 (td, 1 H, *J* = 3.70, 10.47 Hz, H11a), 5.25 (s, 1 H, NH), 6.46 (s, 1 H, H9), 7.06 (s, 1 H, H6), 7.21 (t, 1 H, *J* = 7.31 Hz, H4'), 7.34 (t, 2 H, *J* = 7.56 Hz, H3' and H5'), 7.44 (d, 2 H, *J* = 7.19 Hz, H2' and H6'), 7.57 (s, 1 H, H3) (see Supporting Information for NMR data of **28b–f**).

Biology. K562 Leukemia Cytotoxicity Assay. K562 human chronic myeloid leukemia cells were maintained in RPMI medium supplemented with 10% fetal calf serum and 2 mM glutamine. Then, 190 μ L of K562 suspension (10⁴ cells/mL) was added to each well of columns 2–11 of a 96-well plate, and 190 μ L of medium was added to each well of columns 1 and 12. The compound solution (in 100% DMSO) was serially diluted across a 96-well plate. Each resulting point was then further diluted 1/10 into cell culture medium, and each point was added in triplicate to the cell plate (5% v/v). To cell -ve blanks and compound -ve control wells, 10% DMSO was added at 5% v/v. Assay plates were incubated for 96 h at 37 °C in a humidified atmosphere containing 5% CO₂. Following incubation, 20 μ L of Alamar Blue (1 μ M, final concentration) was added to each well. The plates were then kept for a further 4 h at 37 °C in a humidified atmosphere containing 5% CO₂ and were read at 580–620 nm fluorescence emission using an Envision plate reader. The data were analyzed using GraphPad Prism, and the IC₅₀ values were read as the dose required to reduce the final optical density to 50% of the control value.

DNA Thermal Denaturation Assay. All compounds were stored at $-20\text{ }^{\circ}\text{C}$ under anhydrous conditions prior to use. Stock ligand solutions were freshly prepared in HPLC-grade DMSO, and working solutions were produced by appropriate dilution in aqueous buffer as required. The protocol used to determine thermal denaturation temperatures (T_m) for double-stranded calf thymus DNA and ligand-induced shifts (ΔT_m) has been previously described, together with the analytical procedure.^{44,46,52} Test compounds were subjected to DNA thermal melting (denaturation) studies using calf thymus DNA (CT-DNA, type-I, highly polymerized sodium salt; 42% G + C [Sigma]) at a fixed $100\text{ }\mu\text{M}$ (in DNAP, equivalent to $50\text{ }\mu\text{M}$ in base pairs [bp]) concentration, quantitated using an extinction coefficient of $6600\text{ (M phosphate)}^{-1}\text{ cm}^{-1}$ at 260 nm. This gives a 1:5 [ligand]/[DNAP] ratio. Solutions were prepared in $\text{pH } 7.00 \pm 0.01$ aqueous buffer containing $10\text{ mM NaH}_2\text{PO}_4/\text{Na}_2\text{HPO}_4$ and $1\text{ mM Na}_2\text{EDTA}$ (all AnalaR grade). Working assay mixtures containing CT-DNA and the test compound ($0\text{--}20\text{ }\mu\text{M}$, as required) were incubated at $37.0 \pm 0.1\text{ }^{\circ}\text{C}$ for $0\text{--}72\text{ h}$ using a Grant GD120 water bath. Samples were monitored at 260 nm using a Cary 4000 UV-visible spectrophotometer fitted with a Peltier heating accessory. A precision probe calibrated to $\pm 0.01\text{ }^{\circ}\text{C}$ in the -10 to $+120\text{ }^{\circ}\text{C}$ range was used for temperature measurements. Heating was applied at a rate of $1\text{ }^{\circ}\text{C min}^{-1}$ in the $50\text{--}98\text{ }^{\circ}\text{C}$ range, with optical data sampling at $0.10\text{ }^{\circ}\text{C}$ intervals. A separate experiment was carried out using buffer alone, and this baseline was subtracted from each DNA melting curve before data treatment. Optical data were imported into the Origin 5 program (MicroCal Inc., Northampton, MA) for analysis. DNA helix \rightarrow coil transition temperatures (T_m) were determined at the midpoint of the normalized melting profiles. Results for each compound are shown as the mean \pm standard deviation from at least three determinations. Ligand-induced alterations in DNA melting behavior (ΔT_m) are given by $\Delta T_m = T_m(\text{DNA} + \text{ligand}) - T_m(\text{DNA})$, where the T_m value determined for native CT-DNA is $67.82 \pm 0.07\text{ }^{\circ}\text{C}$ (averaged from ~ 110 runs). Working solutions with the candidate PBDs contained $\leq 0.3\%$ v/v DMSO, and T_m results were corrected for the effects of DMSO cosolvent using a previously described linear correction term determined for calibration mixtures.^{44,52} For kinetic experiments, working solutions of DNA-PBD mixtures at the fixed 5:1 molar ratio were incubated at $37\text{ }^{\circ}\text{C}$ and evaluated after fixed time intervals of 0 (i.e., no incubation), 4 and 18 h. Data were also acquired after incubation for 72 h (not shown).

Molecular Modeling. Molecular modeling studies were performed on a representative set of complexes built using the 9-mer DNA duplex of sequence $d(5'\text{-CGCAGACGC-3'})\cdot d(5'\text{-GCGTCTGCG-3'})$ (Figure 4A) in canonical B-DNA form. Structures for compounds **8**, **12b**, **13a**, and **14l** were built using the HYPERCHEM package (Hyper Inc.), with point-centered charges calculated by a reparameterized version of the AM1 semiempirical method, as implemented in HYPERCHEM. Complexes were built with a covalent bond to the N2 atom of the central guanine nucleotide on the first strand and were initially subjected to molecular-mechanics minimization using the AMBER99⁵³ force field as implemented in HYPERCHEM and a distance-dependent dielectric constant. Sodium counterions were then added to each complex, which were then placed in a TIP3P water box⁵⁴ that extended $\sim 10\text{ \AA}$ from the complex, and further minimizations were performed until a gradient of $< 0.1\text{ kcal \AA}^{-1}\text{ mol}^{-1}$ was reached. Molecular dynamics simulations were then performed under these explicit solvent conditions, with a production run of 5 ns for each complex, during which the total energy was judged to have reached stability. A final round of molecular mechanics minimization was performed on each complex at the end of the dynamics, and the resulting relative energies qualitatively compared with reference to the unsubstituted 2-phenyl compound **8**.

Preliminary energy minimization studies with the **14l** complex were carried out as follows. The 6-quinolinyl substituted ligand (**14l**) was constructed and minimized using the ChemBioOffice

suite of programs (CambridgeSoft), exporting to a PDB format for subsequent conversion to a mol2 format for AMBER using the "antechamber" routine. Gasteiger charges were used, and missing parameters added by means of the "parmchk" program. Covalent binding of each ligand to the C2-NH₂ functional group of the guanine residue of DNA was performed graphically using AMBER "Xleap" utilizing "parm99" and the general Amber force field parameters^{53,55,56} (gaff), maintaining the (S)-configuration at the C11-position of the central PBD ring at the point of attachment to the guanine N2-position. DNA/ligand constructs were exported for subsequent minimization using "Sander" during which the DNA alone was initially restrained with a high force constant, allowing the ligand to adjust to the DNA environment. Further minimization steps were performed while gradually reducing the restraints to zero. The generalized Born/surface area (GB/SA) implicit solvent model was used with monovalent electrostatic ion screening simulated with SALTCON set to 0.2 M. A long-range nonbonded cutoff of 100 \AA was used. To examine the sequence variations of the genomic DNA which would be encountered by the ligand in calf thymus DNA (1:1 adduct), all 16 possible permutations of the two bases upstream of the covalent bond in the guanine of $d(5'\text{-TAXXGATT-3'})\cdot d(5'\text{-AATCYTA-3'})$ were modeled.

Conformational analysis (Figure 4B) with a 14-mer DNA-(**14l**)₂ adduct $[d(5'\text{-AATCTTTAAAGATT-3'})_2]$ was carried out using a previously established procedure.⁴³ Briefly, the conformational search was carried out using the Monte Carlo multiple minimum (MCMM) method and AMBER force field implemented in MacroModel v9.6207.⁵⁷ Two thousand MCMM steps were carried out for each adduct, and the resulting structures analyzed using XCluster and Maestro v8.5207. The position of water molecules around the DNA-(**14l**)₂ adduct was also studied using conformational search. The lowest energy NMR-based structure of the C2-(2-naphthyl) PDB adduct (PDB entry 2k4l) was used as a starting structure for the 1:2 adduct by substituting the relevant C atom on the naphthyl ring with a N atom. The initial structure was solvated using the soak command in the Impact v5.208 software, and the solvated system was subjected to 2000 steps of conformational search as described above.

In Vivo Human Tumour Xenograft Studies. Human tumor xenograft experiments were carried out under a project license issued by the UK Home Office, and UKCCCR guidelines were followed rigorously.⁵⁸ HCT 116 cells (10^7 cells) were injected subcutaneously into the flank of female nu/nu-BALB/c athymic nude mice. Treatment started when xenografts reached $50\text{--}100\text{ mm}^3$. **14l** was prepared in a vehicle of 1% DMSO/saline solution, and control mice were injected with the vehicle only. Animals received **14l** intravenously (iv) at $300\text{ }\mu\text{g/kg}$ as a single dose or $120\text{ }\mu\text{g/kg/d}$ day for five days based on the dosing schedule defined for SJG-136 by Alley and co-workers.²⁴ Weights were monitored daily from the start of treatment (i.e., day 1) to the end of study (i.e., 12 days). Xenograft tumors were measured 3 times a week, and tumor volumes were calculated from calliper measurements as $\text{width}^2 \times \text{length}/2$. Relative tumor volumes (RTVs) were calculated for each tumor by dividing the tumor volume at a specific number of days after the start of treatment by the tumor volume at the start of treatment (day 1) multiplied by 100%. Results are mean \pm SE from 5–10 experiments.

Acknowledgments. Cancer Research UK (C180/A1060 to D.E.T.; C96/A5008 to D.I.J.; C96/A6670 to M.K.) and Spirogen Ltd (U.K.) are thanked for financial support of this work, and the Engineering and Physical Sciences Research Council (GR/R47646/01) is acknowledged for providing a grant for the NMR and MS instrumentation. The authors are grateful to Dr. Emma Sharp for her expert help in preparation of the manuscript.

Supporting Information Available: Full synthetic methodologies, yields, and spectroscopic details for compounds previously published in communication form; synthetic methods,

analytical data: IR, ^1H -, ^{13}C -, 2D-NMR, MS, and HRMS data; optical rotation and HPLC analytical data for all novel C2-substituted PBD-imine compounds reported in the main text; time-course ^1H NMR analyses and MS-MALDI experiments with the sodium bisulfite adducts and DNA-adducts; NCI 60 cell line data for all library members. This material is available free of charge via the Internet at <http://pubs.acs.org>.

References

- Thurston, D. E. Advances in the Study of Pyrrolo[2,1-*c*]-[1,4]benzodiazepine (PBD) Antitumor Antibiotics. In *Molecular Aspects of Anticancer Drug-DNA Interactions*; Neidle, S.; Waring, M. J., Eds.; The Macmillan Press Ltd.: London, 1993; Vol. 1, pp 54–88.
- Thurston, D. E.; Bose, D. S. Synthesis of DNA-Interactive Pyrrolo[2,1-*c*][1,4]benzodiazepines. *Chem. Rev.* **1994**, *94*, 433–465.
- Al-Said, N. H. Facile synthesis of pyrrolo[2,1-*c*][1,4]benzodiazepine-5,11-dione dimer. *J. Heterocycl. Chem.* **2006**, *43*, 1091–1093.
- Baraldi, P. G.; Balboni, G.; Cacciari, B.; Guiotto, A.; Manfredini, S.; Romagnoli, R.; Spalluto, G.; Thurston, D. E.; Howard, P. W.; Bianchi, N.; Rutigliano, C.; Mischiati, C.; Gambari, R. Synthesis, in vitro Antiproliferative Activity, and DNA-Binding Properties of Hybrid Molecules Containing Pyrrolo[2,1-*c*][1,4]benzodiazepine and Minor-Groove-Binding Oligopyrrole Carriers. *J. Med. Chem.* **1999**, *42*, 5131–5141.
- Carlier, P. R.; Zhao, H.; MacQuarrie-Hunter, S. L.; DeGuzman, J. C.; Hsu, D. C. Enantioselective Synthesis of Diversely Substituted Quaternary 1,4-Benzodiazepine-2-ones and 1,4-Benzodiazepine-2,5-diones. *J. Am. Chem. Soc.* **2006**, *128*, 15215–15220.
- Fukuyama, T.; Liu, G.; Linton, S. D.; Lin, S. C.; Nishino, H. Total Synthesis of (+)-Porothramycin-B. *Tetrahedron Lett.* **1993**, *34*, 2577–2580.
- Gauzy, L.; Zhao, R.; Deng, Y.; Li, W.; Bouchard, H.; Chari, R. V. J.; Commercon, A. Cytotoxic Agents Comprising New Tomaymycin Derivatives and Their Therapeutic Use. International Patent WO 2007/085930 A1, **2007**.
- Howard, P. W.; Chen, Z. Z.; Gregson, S. J.; Masterson, L. A.; Tiberghien, A. C.; Cooper, N.; Fang, M.; Coffils, M. J.; Klee, S.; Hartley, J. A.; Thurston, D. E. Synthesis of a Novel C2/C2'-Aryl-Substituted Pyrrolo[2,1-*c*][1,4]benzodiazepine Dimer Prodrug with Improved Water Solubility and Reduced DNA Reaction Rate. *Bioorg. Med. Chem. Lett.* **2009**, *19*, 6463–6466.
- Hu, W.-P.; Liang, J.-J.; Kao, C.-L.; Chen, Y.-C.; Chen, C.-Y.; Tsai, F.-Y.; Wu, M.-J.; Chang, L.-S.; Chen, Y.-L.; Wang, J.-J. Synthesis and Antitumor Activity of Novel Enediyne-Linked Pyrrolo[2,1-*c*][1,4]benzodiazepine Hybrids. *Bioorg. Med. Chem.* **2009**, *17*, 1172–1180.
- Kamal, A.; Rajender; Reddy, D. R.; Reddy, M. K.; Balakishan, G.; Shaik, T. B.; Chourasia, M.; Sastry, G. N. Remarkable Enhancement in the DNA-Binding Ability of C2-Fluoro Substituted Pyrrolo[2,1-*c*][1,4]benzodiazepines and their Anticancer Potential. *Bioorg. Med. Chem.* **2009**, *17*, 1557–1572.
- Kraus, G. A.; Melekhov, A. Synthesis of Pyrrolobenzodiazepines via the PIFA Oxidation of Amines. Synthesis of 8-Deoxy DC-81. *Tetrahedron* **1998**, *54*, 11749–11754.
- Kumar, R.; Lown, J. W. Recent Developments in Novel Pyrrolo[2,1-*c*][1,4]Benzodiazepine Conjugates: Synthesis and Biological Evaluation. *Mini-Rev. Med. Chem.* **2003**, *3*, 323–339.
- Mayer, J. P.; Zhang, J. W.; Bjergarde, K.; Lenz, D. M.; Gaudino, J. J. Solid phase synthesis of 1,4-benzodiazepine-2,5-diones. *Tetrahedron Lett.* **1996**, *37*, 8081–8084.
- Moroder, L.; Lutz, J.; Grams, F.; RudolphBohner, S.; Osapay, G.; Goodman, M.; Kolbeck, W. A New Efficient Method for the Synthesis of 1,4-Benzodiazepine-2,5-dione Diversomers. *Biopolymers* **1996**, *38*, 295–300.
- O'Neil, I. A.; Thompson, S.; Kalindjian, S. B.; Jenkins, T. C. The Synthesis and Biological Activity of C2-Fluorinated Pyrrolo[2,1-*c*][1,4]benzodiazepines. *Tetrahedron Lett.* **2003**, *44*, 7809–7812.
- Purnell, B.; Sato, A.; O'Kelley, A.; Price, C.; Summerville, K.; Hudson, S.; O'Hare, C.; Kiakos, K.; Asao, T.; Lee, M.; Hartley, J. A. DNA Interstrand Crosslinking Agents: Synthesis, DNA Interactions, and Cytotoxicity of Dimeric Achiral Seco-Amino-CBI and Conjugates of Achiral Seco-Amino-CBI with Pyrrolobenzodiazepine (PBD). *Bioorg. Med. Chem. Lett.* **2006**, *16*, 5677–81.
- Rojas-Rousseau, A.; Langlois, N. Synthesis of a New Structural Analogue of (+)-Porothramycin. *Tetrahedron* **2001**, *57*, 3389–3395.
- Tercel, M.; Stribbling, S. M.; Sheppard, H.; Siim, B. G.; Wu, K.; Pullen, S. M.; Botting, K. J.; Wilson, W. R.; Denny, W. A. Unsymmetrical DNA Cross-Linking Agents: Combination of the CBI and PBD Pharmacophores. *J. Med. Chem.* **2003**, *46*, 2132–2151.
- Wang, J.-J. Synthesis of Pyrrolo[2,1-*c*][1,4]benzodiazepine Analogues. U.S. Patent 6,660,856 B2, **2003**.
- Zhou, Q.; Duan, W.; Simmons, D.; Shayo, Y.; Raymond, M. A.; Dorr, R. T.; Hurlley, L. H. Design and Synthesis of a Novel DNA–DNA Interstrand Adenine–Guanine Cross-Linking Agent. *J. Am. Chem. Soc.* **2001**, *123*, 4865–4866.
- Hurlley, L. H.; Reck, T.; Thurston, D. E.; Langley, D. R.; Holden, K. G.; Hertzberg, R. P.; Hoover, J. R. E.; Gallagher, G.; Faucette, L. F.; Mong, S. M.; Johnson, R. K. Pyrrolo[1,4]Benzodiazepine Antitumor Antibiotics—Relationship of DNA Alkylation and Sequence Specificity to the Biological-Activity of Natural and Synthetic Compounds. *Chem. Res. Toxicol.* **1988**, *1*, 258–268.
- Hurlley, L. H.; Thurston, D. E. Pyrrolo(1,4)Benzodiazepine Antitumor Antibiotics—Chemistry, Interaction with DNA, and Biological Implications. *Pharm. Res.* **1984**, *2*, 52–59.
- Thurston, D. E.; Hurlley, L. H. A Rational Basis for the Development of Antitumor Agents in the Pyrrolo[1,4]benzodiazepine Group. *Drugs Future* **1983**, *8*, 957–971.
- Alley, M. C.; Hollingshead, M. G.; Pacula-Cox, C. M.; Wand, W. R.; Hartley, J. A.; Howard, P. W.; Gregson, S. J.; Thurston, D. E.; Sausville, E. A. SJG-136 (NSC 694501), a Novel Rationally Designed DNA Minor Groove Interstrand Cross-Linking Agent with Potent and Broad Spectrum Antitumor Activity. Part 2: Efficacy Evaluations. *Cancer Res.* **2004**, *64*, 6700–6706.
- Hartley, J. A.; Spanswick, V. J.; Brooks, N.; Clingen, P. H.; McHugh, P. J.; Hochhauser, D.; Pedley, R. B.; Kelland, L. R.; Alley, M. C.; Schultz, R.; Hollingshead, M. G.; Schweikart, K. M.; Tomaszewski, J. E.; Sausville, E. A.; Gregson, S. J.; Howard, P. W.; Thurston, D. E. SJG-136 (NSC 694501), a Novel Rationally Designed DNA Minor Groove Interstrand Cross-Linking Agent with Potent and Broad Spectrum Antitumor Activity. Part 1: Cellular Pharmacology, in Vitro and Initial in Vivo Antitumor Activity. *Cancer Res.* **2004**, *64*, 6693–6699.
- Hochhauser, D.; Meyer, T.; Spanswick, V. J.; Wu, J.; Clingen, P. H.; Loadman, P.; Cobb, M.; Gumbrell, L.; Begent, R. H.; Hartley, J. A.; Jodrell, D. Phase I Study of Sequence-Selective Minor Groove DNA Binding Agent SJG-136 in Patients with Advanced Solid Tumors. *Clin. Cancer Res.* **2009**, *15*, 2140–2147.
- Janjigian, Y. Y.; Lee, W.; Kris, M. G.; Miller, V. A.; Azzoli, C. G.; Senturk, E.; Calcutt, M.; Rizvi, N. A.; Phase, I Trial of SJG-136 (NSC/694501) in Advanced Solid Tumors. *Cancer Chemother. Pharmacol.* **2009**, *0*.
- Rahman, K. M.; Thompson, A. S.; James, C. H.; Narayanaswamy, M.; Thurston, D. E. The Pyrrolobenzodiazepine Dimer SJG-136 Forms Sequence-Dependent Intrastrand DNA Cross-Links and Monoalkylated Adducts in Addition to Interstrand Cross-Links. *J. Am. Chem. Soc.* **2009**, *131*, 13756–13766.
- Kaliszczak, M.; Antonow, D.; Patel, K.; Jodrell, D.; Howard, P.; Thurston, D.; Guichard, S. In Pyrrolo[2,1-*c*][1,4]benzodiazepine (PBD) analogues show differential substrate specificity to ABC transporters. AACR Meeting Abstracts, April 12, 2008, Abstract No 3226.
- Aird, R. E.; Thomson, M.; Macpherson, J. S.; Thurston, D. E.; Jodrell, D. I.; Guichard, S. M. ABCB1 Genetic Polymorphism Influences the Pharmacology of the New Pyrrolobenzodiazepine Derivative SJG-136. *Pharmacogenomics J.* **2008**, *8*, 289–296.
- Guichard, S. M.; Macpherson, J. S.; Thurston, D. E.; Jodrell, D. I. Influence of P-glycoprotein Expression on in vitro Cytotoxicity and in vivo Antitumor Activity of the Novel Pyrrolobenzodiazepine Dimer SJG-136. *Eur. J. Cancer* **2005**, *41*, 1811–1818.
- Burger, A. M.; Loadman, P. M.; Thurston, D. E.; Schultz, R.; Fiebig, H.; Bibby, M. C. Preclinical Pharmacology of the Pyrrolobenzodiazepine (PBD) Monomer DRH-417 (NSC 709119). *J. Chemother* **2007**, *19*, 66–78.
- Cooper, N.; Hagan, D. R.; Tiberghien, A.; Ademefun, T.; Matthews, C. S.; Howard, P. W.; Thurston, D. E. Synthesis of Novel C2-Aryl Pyrrolobenzodiazepines (PBDs) as Potential Antitumor Agents. *Chem. Commun.* **2002**, 1764–1765.
- Antonow, D.; Jenkins, T. C.; Howard, P. W.; Thurston, D. E. Synthesis of a Novel C2-Aryl Pyrrolo[2,1-*c*][1,4]benzodiazepine-5,11-dione Library: Effect of C2-Aryl Substitution on Cytotoxicity and Non-Covalent DNA Binding. *Bioorg. Med. Chem.* **2007**, *15*, 3041–3053.
- Antonow, D.; Cooper, N.; Howard, P. W.; Thurston, D. E. Parallel Synthesis of a Novel C2-Aryl Pyrrolo[2,1-*c*][1,4]benzodiazepine (PBD) Library. *J. Comb. Chem.* **2007**, *9*, 437–445.
- Kang, G. D.; Howard, P. W.; Thurston, D. E. Synthesis of a Novel C2-Aryl Substituted 1,2-Unsaturated Pyrrolobenzodiazepine. *Chem. Commun.* **2003**, 1688–1689.
- Leimgruber, W.; Batcho, A. D.; Czajkowski, R. C. Total Synthesis of Anthramycin. *J. Am. Chem. Soc.* **1968**, *90*, 5641–5643.
- Tiberghien, A. C.; Hagan, D.; Howard, P. W.; Thurston, D. E. Application of the Stille Coupling Reaction to the Synthesis of

- C2-Substituted *endo-exo* Unsaturated Pyrrolo[2,1-*c*][1,4]-benzodiazepines (PBDs). *Bioorg. Med. Chem. Lett.* **2004**, *14*, 5041–5044.
- (39) Gregson, S. J.; Howard, P. W.; Corcoran, K. E.; Barcella, S.; Yasin, M. M.; Hurst, A. A.; Jenkins, T. C.; Kelland, L. R.; Thurston, D. E. Effect of C2-*exo* Unsaturation on the Cytotoxicity and DNA-Binding Reactivity of Pyrrolo[2,1-*c*][1,4]benzodiazepines. *Bioorg. Med. Chem. Lett.* **2000**, *10*, 1845–1847.
- (40) Kaneko, T.; Wong, H.; Doyle, T. W.; Rose, W. C.; Bradner, W. T. Bicyclic and Tricyclic Analogs of Anthramycin. *J. Med. Chem.* **1985**, *28*, 388–392.
- (41) Langlois, N.; Rojas-Rousseau, A.; Gaspard, C.; Werner, G. H.; Darro, F.; Kiss, R. Synthesis and Cytotoxicity on Sensitive and Doxorubicin-Resistant Cell Lines of New Pyrrolo[2,1-*c*][1,4]benzodiazepines Related to Anthramycin. *J. Med. Chem.* **2001**, *44*, 3754–3757.
- (42) Thurston, D. E.; Langley, D. R. Synthesis and Stereochemistry of Carbinolamine-Containing Pyrrolo[1,4]Benzodiazepines by Reductive Cyclization of *N*-(2-Nitrobenzoyl)Pyrrolidine-2-Carboxaldehydes. *J. Org. Chem.* **1986**, *51*, 705–712.
- (43) Antonow, D.; Barata, T.; Jenkins, T. C.; Parkinson, G. N.; Howard, P. W.; Thurston, D. E.; Zloh, M. Solution Structure of a 2:1 C2-(2-Naphthyl) Pyrrolo[2,1-*c*][1,4]benzodiazepine DNA Adduct: Molecular Basis for Unexpectedly High DNA Helix Stabilization. *Biochemistry* **2008**, *47*, 11818–11829.
- (44) Jones, G. B.; Davey, C. L.; Jenkins, T. C.; Kamal, A.; Kneale, G. G.; Neidle, S.; Webster, G. D.; Thurston, D. E. The Noncovalent Interaction of Pyrrolo[2,1-*c*][1,4]Benzodiazepine-5,11-Diones with DNA. *Anti-Cancer Drug Des.* **1990**, *5*, 249–264.
- (45) Perry, P. J.; Gowan, S. M.; Reszka, A. P.; Polucci, P.; Jenkins, T. C.; Kelland, L. R.; Neidle, S. 1,4- and 2,6-Disubstituted Amidoanthracene-9,10-dione Derivatives as Inhibitors of Human Telomerase. *J. Med. Chem.* **1998**, *41*, 3253–3260.
- (46) Gregson, S. J.; Howard, P. W.; Gullick, D. R.; Hamaguchi, A.; Corcoran, K. E.; Brooks, N. A.; Hartley, J. A.; Jenkins, T. C.; Patel, S.; Guille, M. J.; Thurston, D. E. Linker Length Modulates DNA Cross-Linking Reactivity and Cytotoxic Potency of C8/C8' Ether-Linked C2-*exo*-Unsaturated Pyrrolo[2,1-*c*][1,4]benzodiazepine (PBD) Dimers. *J. Med. Chem.* **2004**, *47*, 1161–1174.
- (47) Thurston, D. E.; Bose, D. S.; Howard, P. W.; Jenkins, T. C.; Leoni, A.; Baraldi, P. G.; Guiotto, A.; Cacciari, B.; Kelland, L. R.; Foloppe, M. P.; Rault, S. Effect of A-ring Modifications on the DNA-Binding Behavior and Cytotoxicity of Pyrrolo[2,1-*c*][1,4]benzodiazepines. *J. Med. Chem.* **1999**, *42*, 1951–1964.
- (48) Chen, Z. Z.; Gregson, S. J.; Howard, P. W.; Thurston, D. E. A Novel Approach to the Synthesis of Cytotoxic C2-C3 Unsaturated Pyrrolo[2,1-*c*][1,4]benzodiazepines (PBDs) with Conjugated Acrylyl C2-Substituents. *Bioorg. Med. Chem. Lett.* **2004**, *14*, 1547–1549.
- (49) Gregson, S. J.; Howard, P. W.; Barcella, S.; Nakama, A.; Jenkins, T. C.; Kelland, L. R.; Thurston, D. E. Effect of C2/C3-*Endo* Unsaturation on the Cytotoxicity and DNA-Binding Reactivity of Pyrrolo[2,1-*c*][1,4]benzodiazepines. *Bioorg. Med. Chem. Lett.* **2000**, *10*, 1849–1851.
- (50) Guichard, S.; Arnould, S.; Hennebelle, I.; Bugat, R.; Canal, P. Combination of oxaliplatin and irinotecan on human colon cancer cell lines: activity in vitro and in vivo. *Anti-Cancer Drugs* **2001**, *12*, 741–751.
- (51) Guichard, S. M.; Macpherson, J. S.; Mayer, I.; Reid, E.; Muir, M.; Dodds, M.; Alexander, S.; Jodrell, D. I. Gene expression predicts differential capecitabine metabolism, impacting on both pharmacokinetics and antitumour activity. *Eur. J. Cancer* **2008**, *44*, 310–317.
- (52) McConnaughie, A. W.; Jenkins, T. C. Novel Acridine-Triazines as Prototype Combilexins – Synthesis, DNA-Binding, and Biological Activity. *J. Med. Chem.* **1995**, *38*, 3488–3501.
- (53) Cornell, W. D.; Cieplak, P.; Bayly, C. I.; Gould, I. R.; Merz, K. M.; Ferguson, D. M.; Spellmeyer, D. C.; Fox, T.; Caldwell, J. W.; Kollman, P. A. A 2nd Generation Force-Field for the Simulation of Proteins, Nucleic-Acids, and Organic-Molecules. *J. Am. Chem. Soc.* **1995**, *117*, 5179–5197.
- (54) Jorgensen, W. L.; Chandrasekhar, J.; Madura, J. D.; Impey, R. W.; Klein, M. L. Comparison of Simple Potential Functions for Simulating Liquid Water. *J. Chem. Phys.* **1983**, *79*, 926–935.
- (55) Case, D. A.; Cheatham, T. E.; Darden, T.; Gohlke, H.; Luo, R.; Merz, K. M.; Onufriev, A.; Simmerling, C.; Wang, B.; Woods, R. J. The Amber Biomolecular Simulation Programs. *J. Comput. Chem.* **2005**, *26*, 1668–1688.
- (56) Pearlman, D. A.; Case, D. A.; Caldwell, J. W.; Ross, W. S.; Cheatham, T. E.; Debolt, S.; Ferguson, D.; Seibel, G.; Kollman, P. Amber, a Package of Computer-Programs for Applying Molecular Mechanics, Normal-Mode Analysis, Molecular-Dynamics and Free-Energy Calculations to Simulate the Structural and Energetic Properties of Molecules. *Comput. Phys. Commun.* **1995**, *91*, 1–41.
- (57) Mohamadi, F.; Richards, N. G. J.; Guida, W. C.; Liskamp, R.; Lipton, M.; Caufield, C.; Chang, G.; Hendrickson, T.; Still, W. C. MacroModel—An Integrated Software System for Modeling Organic and Bioorganic Molecules Using Molecular Mechanics. *J. Comput. Chem.* **1990**, *11*, 440–467.
- (58) Workman, P.; Twentymen, P.; Balkwill, F.; Balmain, A.; Chaplin, D.; Double, J.; Embleton, J.; Newell, D.; Raymond, R.; Stables, J.; Stephens, T.; Wallace, J. United Kingdom Co-ordinating Committee on Cancer Research (UKCCCR) Guidelines for the Welfare of Animals in Experimental Neoplasia (2nd Edition). *Br. J. Cancer* **1998**, *77*, 1–10.
- (59) Masterson, L. A.; Spanswick, V. J.; Hartley, J. A.; Begent, R. H.; Howard, P. W.; Thurston, D. E. Synthesis and Biological Evaluation of Novel Pyrrolo[2,1-*c*][1,4]benzodiazepine Prodrugs for Use in Antibody-Directed Enzyme Prodrug Therapy. *Bioorg. Med. Chem. Lett.* **2006**, *16*, 252–256.